SEPTEMBER 2023 M.Sc. in Civil Engineering MOHAMMED OBAID

REPUBLIC OF TÜRKİYE

GAZİANTEP UNIVERSITY

GRADUATE SCHOOL OF NATURAL & APPLIED SCIENCES

SIMULATION OF SCOURING AROUND BRIDGE PIER BY USING HEC-RAS

M.Sc. THESIS

in

CIVIL ENGINEERING

BY

MOHAMMED ALI OBAIED

SEPTEMBER 2023

`

SIMULATION OF SCOURING AROUND BRIDGE PIER BY USING HEC-RAS

M.Sc. Thesis

in

Civil Engineering

Gaziantep University

Supervisor

Assist. Prof. Dr. Ayşe Yeter GÜNAL

Co-Supervisor

Prof. Dr. Raad Hoobi IRZOOKI

BY

Mohammed Ali OBAIED

SEPTEMBER 2023

`

`

SIMULATION OF SCOURING AROUND BRIDGE PIER BY USINGHEC-RAS

Submitted by **Mohammed OBAID** in partial fulfillment of the requirements for the degree of Master of Science in **Civil Engineering, Gaziantep University** is approved by,

Prof. Dr. Çiğdem AYKAÇ
Director of the Graduate School of Natural and Applied Sciences. ………….............

Prof. Dr. Nildem TAYŞİ
Head of the Department of Civil Engineering ………….............

Asst. Prof. Dr. Ayşe Yeter GÜNAL
Gaziantep University ………….............

Exam Date: 15 September 2023

Examining Committee Members:

Asst. Prof. Dr. Ayşe Yeter GÜNAL
Gaziantep University ………….............

Prof. Dr. Aytaç GÜVEN
Gaziantep University ………….............

Assoc. Prof. Dr. Ali AYTEK
Gaziantep Islam Science and Technology University ………….............

`

I hereby declare that all information in this document has been obtained and presented in accordance with academic rules and ethical conduct. I also declare that, as required by these rules and conduct, I have fully cited and referenced all material and results that are not original to this work.

Mohammed Ali OBAIED

ABSTRACT

SIMULATION OF SCOURING AROUND BRIDGE PIER BY USING HEC-RAS

OBAIED, Mohammed Ali
M.Sc.in Civil Engineering

Supervisor: Assist. Prof. Dr. Ayşe Yeter GÜNAL
Co-Supervisor: Prof. Dr. Raad Hoobi IRZOOKI

September 2023
75 pages

Bridges are crucial components of our transportation system and pricey highway hydraulic structures. One of the risky issues in river engineering is erosion induced by the flow around the piers of these structures in alluvial streams, and the scour around bridge piers is one of the circumstances that has drawn a lot of attention. Numerous bridge collapses have happened as a result of the weakening of their foundations. In this study, we used the (HEC-RAS) program in order to simulate previous practical experiments and demonstrate the possibility of using the program to learn about scouring around bridge piers, and compared the results of the program (HEC-RAS) with the results of scouring for practical experiments. The greatest value of scouring for the (HEC-RAS) programmed was (50) mm at a diameter of (50) mm and a discharge of (40) l/sec, while the lowest value was (30) mm at a diameter of (25) mm and a discharge of (20) l/sec, and the percentage of increase being in scoring (40%). The maximum values for scouring and the lowest values were at the same diameters and discharge for simulation (63 - 25) mm, respectively, in the real experiments for which the simulated process was run on the programmed. In addition, at the pavement with a diameter of (25) mm, the increase in discharge from (20 to 40) liters / second led to the stability of scouring (30) mm, and the scouring depth increased from (40 to 50) mm at the pier with a diameter of (50). mm, that is, the percentage of increase was equal to (20%), we conclude that the increase in the diameter of the pier and the increase in flow leads to an increase in the depth of scouring.

Keywords: Bridge pier, HEC-RAS, Scouring.

ÖZET

HEC-RAS KULLANARAK KÖPRÜ İSKELESİ ÇEVRESİNİ OYMA SİMÜLASYONU

OBAIED, Mohammed Ali
Yüksek Lisans Tezi, İnşaat mühendisliği
Danışman: Dr. Öğr. Üyesi . Ayşe Yeter GÜNAL
İkinci Danışman: Prof. Dr. Raad Hoobi IRZOOKI
Eylül 2023
75 sayfa

Köprüler, ulaşım sistemimizin ve pahalı karayolu hidrolik yapılarımızın çok önemli bileşenleridir. Akarsu mühendisliğindeki riskli konulardan biri de alüvyal akarsularda bu yapıların ayaklarının etrafındaki akışın neden olduğu erozyondur ve köprü ayaklarının etrafındaki oyulma çok dikkat çeken durumlardan biridir. Temellerinin zayıflaması sonucu çok sayıda köprü yıkılmıştır. Bu çalışmada, daha önceki uygulamalı deneyleri simüle etmek ve köprü ayakları etrafında oyulmayı öğrenmek için programın kullanılabileceğini göstermek amacıyla (HEC-RAS) programını kullandık ve programın sonuçlarını (HEC-RAS) programın sonuçlarıyla karşılaştırdık. Programlanan (HEC-RAS) için en büyük oyulma değeri (50) mm çapta (50) mm ve (40) l/sn'lik bir deşarj olurken, en düşük değer (30) mm çapında (30) mm idi. (25) mm ve (20) l/sn boşaltma ve oyulmadaki artış yüzdesi (%40). Simüle işlemin programda yürütüldüğü gerçek deneylerde, oyulma için maksimum değerler ve simülasyon için boşaltma için aynı çaplarda (63 - 25) en düşük değerler sırasıyla mm olmuştur. Ayrıca (25) mm çapındaki kaplamada, (20) litre/sn'den 40 litreye debi artışı, oyulma stabilitesinin (30) mm olmasına ve oyulma derinliğinin (40'tan 50'ye) çıkmasına neden olmuştur. (50) çapında iskelede mm. mm, yani artış yüzdesi (%20)'ye eşitti, ayak çapındaki artışın ve akıştaki artışın oyulma derinliğinde bir artışa yol açtığı sonucuna vardık.

Anahtar Kelimeler: Köprü ayağı, HEC-RAS, Oyulma.

''Dedicated to my family''

ACKNOWLEDGEMENTS

I would like to thank my supervisor, Assist. Prof. Dr. Ayşe Yeter GÜNAL and Co-Supervisor: Prof. Dr. Raad Hoobi IRZOOKI for his guidance and support throughout the study. I am thankful for his encouragement and motivation. I would like to express my love and gratitude to my family for their support, always best wishes.

TABLE OF CONTENTS

LIST OF TABLES

LIST OF FIGURES **page**

LIST OF SYMBOLS

Notations	Definitions
b	Width of the cannel.
D	Diameter of the pier nose.
D. 50	Mean of the soil size particle.
D. p	Diameter of circular pier.
d. s	Maximum scour depth.
F. r	Froude number.
G_s	Specific gravity of the bed soil material.
g	Gravitational acceleration.
H	Height of the flow over the weir crest.
K. p	The ratio between the length of pier to the diameter of the nose.
L1, L2, L3	Lengths of the piers.
Q	Discharge of the cannel.
Re D	Reynolds number.
R^2	The coefficient of determination of the equation.
v	Velocity of flow.
vc	Critical velocity of flow.
X	Distance between tow piers.

y Depth of water from the surface of bed soil material.

α Angle of attack of pier to flow, in the horizontal plane.

ρ.s Density of the sediment.

ρ_w Density of the water.

LIST OFABBREVIATIONS

CSU	Colorado State University Equation.
HEC-RAS	The Hydrologic Engineering Center's River Analysis System.
RANS	Reynolds Averaged Navier-Stokes Equations.
RNG	Renormalize Group Theory.
SOR	Successive Over-Relaxation.
SPSS	Statistical Package for the Social Sciences.

CHAPTER 1

INTRODUCTION

1.1 General

Bridges are crucial components of our transportation system and pricey highway hydraulic structures. One of the risky issues in river engineering is erosion induced by the flow around the piers of these structures in alluvial streams, and the scour around bridge piers is one of the circumstances that has drawn a lot of attention. Numerous bridge collapses have happened as a result of the weakening of their foundations; one such instance is the Tuz Bridge in Iraq's Salahalddin Province, see Figure (1-1).

Figure 1.1 Failure of settlement in one of the piers of Tuz bridge in Salahdin.

When constructing these structures, attention must be given because bridges frequently have an impact on rivers that are in motion. Therefore, a number of criteria must be acknowledged and taken into explanation in order to lower the anticipated risks of failure, including choosing the right spot for the bridge, hydraulic qualities (Average flow rate at the bridge's opening and scour depth at the piers' bases), modifications to the channel, hydrological information (such as the frequency of floods and the elevation-runoff curve), and the size and design of the bridge pier (Jansen, et.al. 1982).

Due to the unsteady flow in many directions, the maximum depth of scouring happens when a river floods. The maximum scour prediction at the piers must be adopted in the project of the bridge piers in order to ensure safety conditions and economical design, in order to determine the proper foundation depth, and avoid minatory of the structure's stability.

One method of determining the length of the bridge and the minimal space between piers (the superstructure's restrictions on the choice of pier geometry structural consideration, pier type, loading, and soil carrying capacity) is a projection of the magnificent scour that floods will produce, as well as backwater's effect. Utilizing short bridges saves money, yet also creates backwaters. The riverfront area in front of the bridge is damaged by floods that occur repeatedly. Therefore, it is significant to consider the height of the upstream portion of the bridge. In fact, relief bridges rather than earthen approaches can be built in the flood plain to lessen the impacts of backwater. By figuring out the maximum depth of the scouring, the designer is interested in figuring out the size and depth of the pier foundation. Therefore, the majority of research focuses on calculating the maximum depth of scrub that the flow might reach if enough time has passed (Mousavi & Daneshfaraz, 2013).

A great deal of progress has been made in understanding the mechanics of the erosion process and developing various methodologies to predict the maximum expected local erosion depth at bridge abutments thanks to scientific development. As a result, supporting tools were made available to hydraulic engineers to help them choose the proper bridge foundations throughout the design phase. Additionally, a number of techniques have been developed to lower excavation depth to safe levels, and engineers and researchers have accepted these techniques. Changing the design of the pier section to be more streamlined to prevent runoff, for example, by using engineering details, or work to divert the flow away from the abutment by adding other facilities that protect the soil of the river bed around the abutment.

1.2 Aims of the Study

This study's primary objectives are:

1. The aim of this study is to evaluate the possibility of using the HEC-RAS program to find out the amount of scouring around bridge piers.
2. Compare practical results obtained in the laboratory with program results.

3. By using the program, we may help save time and money by knowing the amount of scouring around piers.
4. A statement of the effect changes in the diameter of piers on the depth scouring around these piers and the different drainages of the runoff.
5. Investigating the effect of distances between the piers on the depth of the scouring around these piers.
6. Work on deriving a situational equation to calculate the highest scouring that occurs around the circular piers, depending on the variables affecting the depth of this scour.

1.3 Limitations of the Study

The following are some of the study's limitations:

1. Clear water condition.
2. A single and multiple circular piers with diameters (62, 36, 21) mm.
3. Using rectangular supports with semi-circular ends and lengths (7D, 9D, 11D) from the face of the anterior of the abutment to the posterior face, where (D) represents the semicircular end diameter.
4. Four sediment grain sizes were used (D_{50}=0.3-0.6mm).
5. Flow discharge varied from (20 to 40) l/s, where each run will carried out under subcritical flow conditions.

1.4 Thesis Layout

A brief summary of each of the thesis' four chapters is given below:

Chapter One offers a summary of the study's goals, limitations, and issues with scouring near bridge piers. Chapter Two provides historical context, a synopsis of prior new and numerical studies on scrub about the bond pier. Chapter Three includes a complete background on the program (HEC-RAS), how the program works, and removing results. Chapter Four comprises showing and deliberating both theoretical and laboratory results, as well as using a technique to lessen scouring. Chapter Five the key findings and suggestions of this research.

CHAPTER 2

LITERATURE REVIEW

2.1 Introduction

In this chapter, various studies have been approved to investigate the phenomenon of local scouring at Bond Pier. These studies have explored several factors, such as the size of bottom atoms, dissimilar movement conditions, and the form and sizes of the pier. Despite the existing research, this chapter aims to provide comprehensive definitions and a thorough review of the literature related to the subject of local scouring at the bridge pier.

2.2 The Scour

Scouring poses a significant problem that undermines the stability of bridge foundations. There are three primary forms of scouring observed at bridge supports: general scouring, concentric scouring, and local scouring. Moreover, Cheremisinoff (Ali & Ghazali, 2013) has classified scour into two fundamental categories: general scour and local scour. Additionally, Melville and Coleman have further categorized scour based on the illustration shown in Figure (B. W. Melville & Coleman, 2000) (1-2).

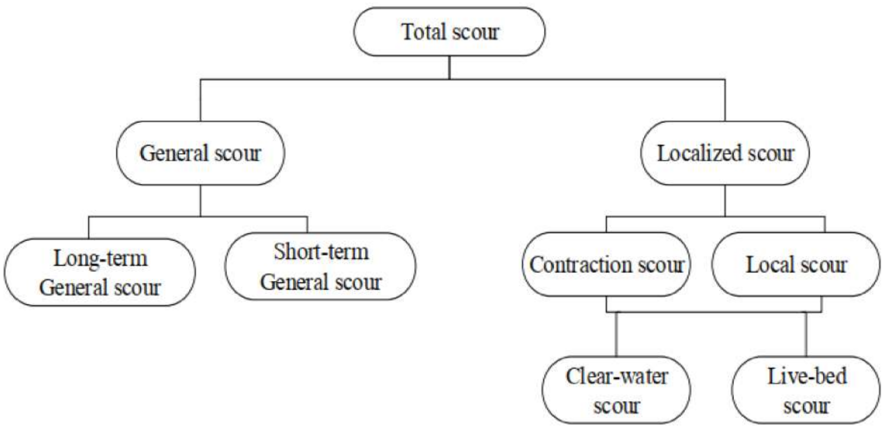

Figure 2.1 Separated the scour (Melville and Coleman, 2000)

2.3 Types of Scours

The erosion phenomenon can be clarified as shadows:

1. Natural scouring: This type of scouring occurs naturally over extended periods due to various factors. It can be reason by the river's changing form, degradation over time, or the relocation of bedforms. It may also result from the unstable of melting streams, which can be influenced by geological procedures or human-made structures. Whether or not a bond exists, usual scouring takes place gradually and over a considerable span of time.
2. General scour: General scouring can occur when the watercourse is constrained, causing the flow to be concentrated and pass through the piers and earthen approaches. As the waterway narrows, the average flow velocity increases, leading to higher shear forces. Consequently, the bed physical is eroded to widen the watercourse and reinstate speed balance. However, once the shave force surpasses the critical drag power, the scouring process stops.
3. Local scour: This type of scouring refers to a drop in the riverbed level that occurs near an obstruction due to the uneven course of the three-dimensional water flow and the disturbances caused by obstacles such as piles, bridge piers, and dams. It's important to note that different forms of scour can happen simultaneously. Thus, considering multiple influences is crucial in determining the maximum scour depth. In most cases, an additive relationship is recommended to account for various scour types, except in situations where the presence of one type may significantly affect another (Moncada-M, Aguirre-Pe, Bolivar, & Flores, 2009).

2.3.1 Scour Hole Formation

Figure (2-2) shows the flow of sand around a split pier, with regions I and II representing specific areas where the soil movement occurs based on their respective locations and directions.

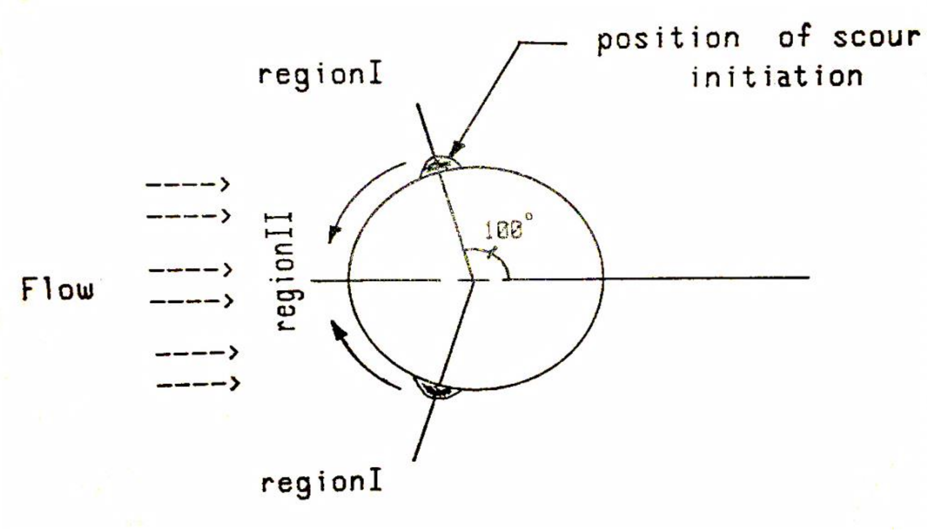

Figure 2.2 Position of Initial Scour.

Erosion initiates in zone I, where high local velocities lead to the rapid scouring of the leading edges of small holes. As these holes enlarge, they converge in zone II, resulting in a symmetrical area of scrub about the pier's longitudinal axis. Laboratory experiments have shown that this development can occur in less than a minute (Ettema, Melville, & Barkdoll, 1998). Hannah (1993) discovered that the uppermost velocity for a cylinder equestrian to a flat plate happens at an angle of approximately 100 degrees to the approaching flow. The scrub hole may initially be localized at the pier's nose or continuously encircle it. However, over time, the scouring will feast until equilibrium is achieved. In the area surrounding an obstruction upstream, a truncated cone-shaped scour hole with a slope matching the sediment's angle of rest and a round bottom can be formed due to the scouring action. At the downstream portion of the scour hole, two tail rises are shaped with a flatter slope than the angle of rest (Raudkivi & Ettema, 1977).

2.3.1 Factors Affecting Local Scour

The scour phenomenon involves several factors that can pique interest, some of which are challenging to measure:

- **Pier and Bridge Geometry:**

a) Absolute and relative size of piers concerning the canal width.

b) Number of piers and their spacing.

c) Bridge positioning relative to the channel axis.

d) Pier orientation concerning the flow direction (angle of attack in the horizontal plane) over the bridge's expected lifespan.

e) Vertical plane angle of attack.

- **Stream-related Parameters (Hydrology and Channel Geometry):**

a. Discharge characteristics and fluid properties, such as viscosity and density.

b. Flood features and incidence rates.

c. Flow depths at different discharges.

d. Motion and pattern of velocity.

e. Channel and flow alignment both upstream and downstream of the crossing.

f. Cross-sectional form of the channel.

g. Channel gradient (stream slope).

h. Overbank considerations, including the impact on the principal channel or concentration of flood flows.

i. The presence of debris carried by the water.

j. These parameters vary significantly over time and are heavily assessed by the designer's discretion.

- **Stream Bed Silt Criteria:**

a. Type of bed material, including its shape, packing, and weight.

b. Size and distribution of bed material sizes.

These factors collectively influence the scouring process and require careful consideration during the design and evaluation of bridge structures to ensure their long-term stability and safety.

2.4 Historical Background

Bridge failures during severe flooding are a significant concern in many countries, and scour is identified as one of the major contributing factors to such failures (B. W. Melville & Coleman, 2000). Scour can be a result of human activities or environmental changes. Notably, areas vulnerable to hurricanes and annual floods, particularly in the Middle East, have reported numerous accidents involving bridge failures (Lu, Hong, Su, Wang, & Lai, 2008). Statistics reveal that approximately 60% of bridge failures in the United States are caused by scour (source not mentioned). E.g., during the spring floods of 1987, 17 bridges in the United States and England were damaged, while 73 bridges in Pennsylvania and Virginia, USA, were destroyed by floods in 1985. A detailed investigation by the US Department of Transportation from 1962 to 1974 revealed damages totaling USD 100 million. Given the significant material and human losses resulting from bridge failures, it is imperative to conduct focused studies on the scour around bridge piers. Prioritizing countermeasures to mitigate scour is essential (Grimaldi, Gaudio, Calomino, & Cardoso, 2009). Researchers have been working on emerging reckonings and approaches to address the scour problem since the 1950s. Most of the future formulations for decisive scour depth are based on laboratory experiments, sometimes complemented by field findings. By conducting laboratory experiments and investigating the influence of various variables, researchers have discovered approximate formulas to approximate the maximum depth of scour (Lagasse, 2007).

2.5 Literature Review

In this study, the researchers investigated the impact of dune on riprap and the consequences of the riprap layer's location on the bottom floor. The experiment was led in a live bed with soil having a D50 (median particle size) of 0.95 mm. The critical shear velocity was calculated using Shields' function, and the trials were conducted over a continuous 24-hour period with a constant flow. The responses of the riprap layer were experiential at various movement velocities relative to the critical approach velocity of the riprap layer. The result designated that in the presence of a mobile bed, the effectiveness of riprap could be enhanced by cumulative the width of riprap atoms (Lauchlan & Melville, 2001). This finding suggests that larger riprap particles may offer better protection against the impact of dunes and contribute to improved stability and performance of the riprap layer in preventing erosion and scour.

The study examined the influence of various collar forms fixed at different heights and slopes to encircle rectangular piers. Each trial was led in a channel that was filled halfway with sand, where the median particle size (D50) of the sand was 1mm. Prior to the main experiments, some initial tests were approved out to gather the necessary prerequisites for the study.

Laboratory tests were then performed using a specialized instrument with an exactness of 0.1 mm to measure and quantify the depth of the scour. The research findings revealed that as the flow inclination angle increased, the efficiency of the collar decreased. Additionally, the study concluded that the collar design was more effective around rectangular piers compared to circular piers. This efficiency was attributed to the fact that the downstream scour did not spread the upstream edge of the collar surrounding the rectangular piers. This design feature played a significant role in reducing scour and protecting the piers effectively.

Helical wires are commonly used in modern construction practices for piers submerged in waves. In Figure (2-3), different combinations of cable-to-pier diameter ratios and thread angles (α) are analyzed for single, double, and triple-threaded piles. The study was led below clear water and stay-bed conditions, using uniform sand in experimental tests. To monitor flow discharge, a calibrated V-notch weir was employed, and 3D velocities were determined using an acoustic Doppler velocimeter with a 5 cm probe head. The research revealed that the helical wires effectively reduced the strength of the horseshoe vortex and downflow beneath the waves. Among the configurations tested, the ratio of 0.75 cable-to-pier diameter was found to be the most effective. The most significant reduction in scour depth, approximately 46.3%, was observed in the case of a triple-threaded pile with a 15° thread angle under constant flow conditions (Dey, Sumer, & Fredsøe, 2006). These findings highlight the beneficial impact of helical wires in mitigating scour around submerged piers and improving their stability in wave environments.

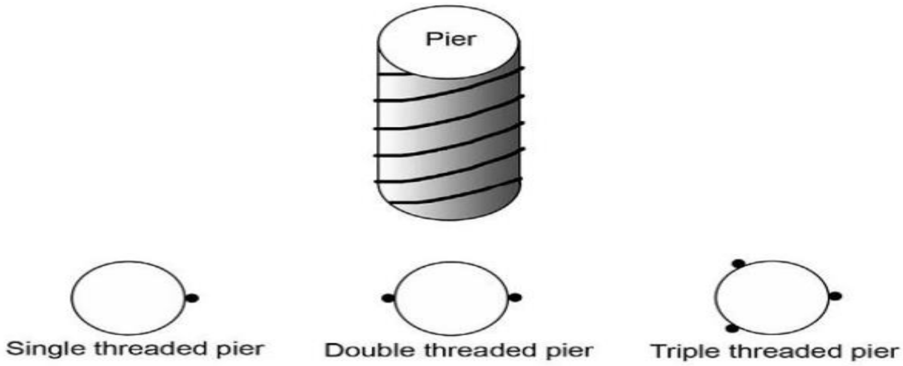

Figure 2.3 Overall View of The Spirally Wired Pier (Dey et al., 2006).

The researchers conducted an experimental investigation on scour near the abutment using a hydraulic channel with transparent walls. The channel was 28.5 meters long, 1.5 meters wide, and had a slope of 0.001. A section of 5.8 meters of the channel was excavated and filled with earthen ground to a depth of 0.48 meters in the flow direction. The channel had a pump with a fixed tank attached to control various flow rates, and a control gate was installed at the channel's end for discharge adjustment. Plexiglas piers of different lengths (40, 35, 30, 25, 20, and 15 cm) with a constant width of 10 cm were used in the experiments. A sharp-crested rectangular weir was constructed at the upstream section of the flume to measure flow discharge. Measures were taken to reduce eddies and flow turbulence at the canal entry using bricks and a screen. Stable flow conditions were essential for accurate measurement of weir water depth and scour depth around the piers. The researchers employed a point gauge with millimeter accuracy to measure the maximum scour depths without affecting the scour area's shape. Additionally, a sound device (Sea Tek 5 MHz Ultrasonic Ranging System) was used to obtain three-dimensional coordinates representing the erosion area surrounding the support.

In total, 60 trials were conducted, with 54 trials lasting three hours each on piers of various lengths and three different abutment positions. Collar widths of 5, 7.5, and 10 cm were used to evaluate their effectiveness in achieving maximum scour depths around the abutments. Six additional trials were conducted with the same abutments but without collars for comparison, The aim was to determine the most effective collar configuration and its impact on scour depths and pier stability (Kumar, Yadav, & Himanshu, 2011).

In the study conducted by Kumar, Yadav, and Himanshu in 2011, water surface profiles surrounding a bridge pier were analyzed using a one-dimensional hydraulic model, such as the HEC-RAS (Corps of Engineers) model. By calculating the depth of scour during the design phase, the cost of constructing bridge foundations can be significantly reduced. Assessing scour is essential in developing innovative, feasible, and cost-effective countermeasures when designing new bridges or reconstructing existing ones.

The research findings indicated the following relationships:

- Critical velocity increases with particle size.
- Scour depth increases with bed roughness.
- Local scour depth decreases with increasing pier inclination angle.

These results provide valuable insights into the factors influencing scour and can aid in making informed decisions to enhance the stability and durability of bridge foundations.

In this study, the researchers investigated local scour using the CSU and Froehlich equations and employed HEC-RAS software to analyze the results. A comparison was made between human and computerized calculations of these equations to establish similar hydrological and hydraulic conditions. The researchers compared the results of empirical formulas and HEC-RAS in the scattered length of the Haraz River, as depicted in Figure (2-4), which shows the schematic plan of the river, bridge, and scour depth. The study observed significant changes in the parameters' results, which were influenced by examining the Froude number and how it was measured, along with the effective coefficients of popular empirical formulas and software. The researchers found that HEC-RAS equations can yield useful outcomes when their coefficients are analyzed with sufficient engineering precision and a controlled approach to the use or non-use of coefficients within specified boundaries. In conclusion, the study highlights the importance of analyzing the coefficients in empirical formulas and software to obtain accurate and reliable results for local scour assessment (Mousavi & Daneshfaraz, 2013). A thorough engineering perspective and careful consideration of the Froude number are essential for obtaining meaningful findings from HEC-RAS equations.

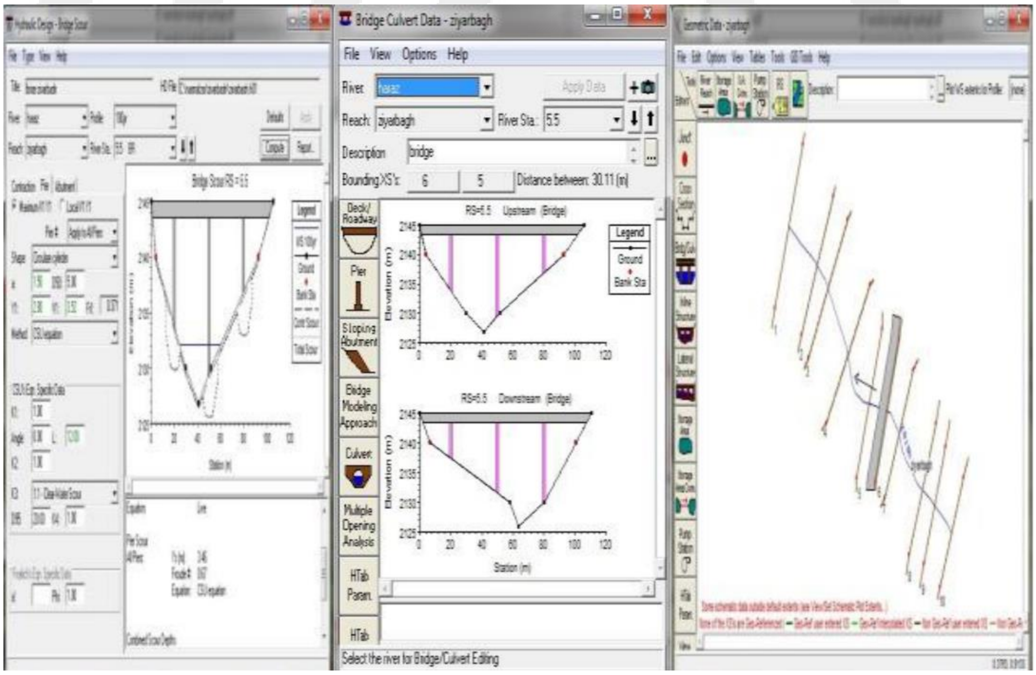

Figure 2.4 Schematic Plan of River, Bridge, and Scour Depth.

In this study, the researchers investigated the scour about the pier of a bridge's foundation. The experiments were led in a tilting flume with dimensions of 16 m in length, 1 m in width, and 1 m in depth, having a constant longitudinal slope of 0.001. The flume was installed in the Hydraulics Laboratory of the University of Malaya.

The working part of the flume, measuring 4.4 meters, was located in the middle, and a control block was used to modify the span where the physical model was placed. The flume was filled with uniform sediment material with a diameter of 0.8 mm to nadirs of 20 cm inside the control block and 5 cm outside the control block. A model of the bridge's substructure was created using an 8 cm long real pier with 5 cm width piles. The maximum diameter of the pier or piling was fixed at 10 percent of the flume breadth (25 cm), following Chiew and Melville's recommendations to stop wall influences on the scour rate. The geometry of the bridge's infrastructure is exposed in Figure (2-5).

Shields' figure was used to approximate the critical shave velocity (Uc) of the bed material, while Melville and Coleman's formulas were primarily working to control the critical flow speed (Uc) for residue entrainment. The experiments were conducted in clean water, with a verge flow strength of (U/Uc=0.95), where U is the average approach flow speed. Thus, the flow degree was reliably fixed at 0.345 m/s in all trials, and the comparative complexity of flow used for every assessment was 35 cm. The study revealed that investigative an exposed pile resulted in an incessant upsurge in the scour depth, which was produced by the presence of an active talisman vortex around the exposed pile. The horseshoe-shaped vortex in front of the pile led to a deeper scour depth (Akib, Liana Mamat, Basser, & Jahangirzadeh, 2014). These findings provide valuable insights into the scouring patterns and dynamics around bridge piers, contributing to a better understanding of bridge foundation stability in river environments.

Figure 2.5 A model of Bridge Piers In the Laboratory.

Researchers investigate the local scour about bridge piers of various forms using the Hydrologic Engineering Center River Analysis System (HEC-RAS) software. The HEC-RAS model, utilizing the CSU equation as a default, proved to be a valuable tool for estimating the scour depth for bridge piers. The results indicated that the square-shaped pier exhibited the highest calculated scrub depth value, while the part about the sharp-nosed dock had a larger value. Scrub depth values were found to be similar for the circular pier, rounded nose, and the pier with a group of cylinders. Figure (2-6) displays the hydraulic data on pier scour. These findings contribute to the understanding of local scour patterns around different bridge pier shapes and demonstrate the effectiveness of HEC-RAS software in estimating scour depth, providing valuable insights for bridge design and stability assessments (Jalil, 2018).

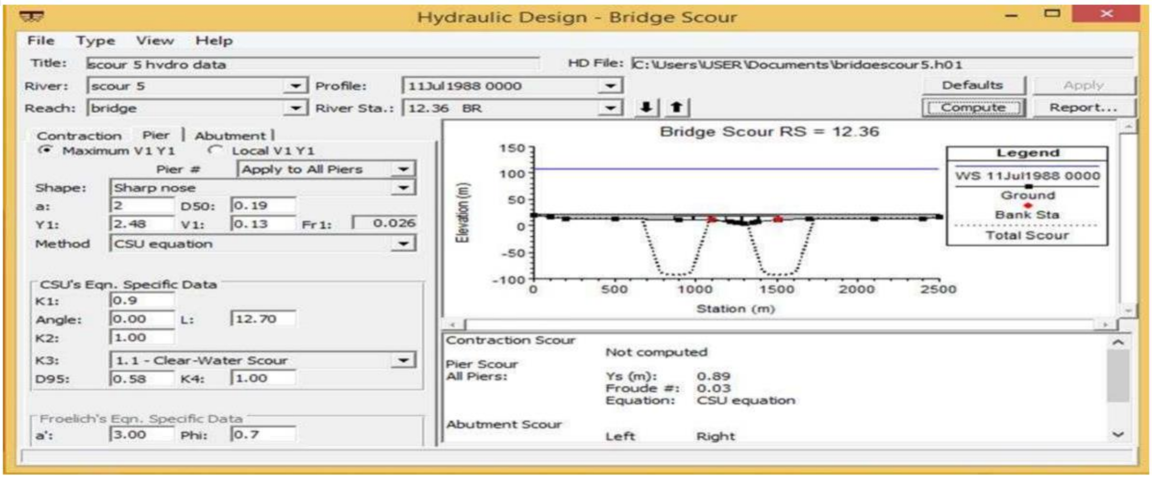

Figure 2.6 Hydraulic Data Pier Scour

In this experimental study, researchers inspected the scrub around a rotund pile in a recirculating channel with dimensions of 4 meters in length, 40 centimeters in width, and 20 centimeters in depth. At the channel's entrance, gravels of various sizes were located to reduce disturbance. The experiments were led in a spotless water setting, with a nasty width of sand size (D50) at 1.5 mm. A 7.0 cm-diameter circular pile was placed in the center of the canal. The study included different pile configurations, which had perforated sacrificial piles with varying hollow diameters (d2) of 0.25, 0.43, and 0.6 of the pile's diameter. There were a total of 80 experimental runs, considering various water depths and pile characteristics. All runs continued for two hours, throughout which 95% of the maximum scour occurred. The relationship between the greatest scour depth (ds) and the time (T) is portrayed in Figures 2–7. According to

Mohamed et al. (2016), the use of a sacrificial pile with a diameter of 0.33D at a location four times the diameter of the pile resulted in a reduction of 89% in the scour depth during the two-hour duration. These findings have practical implications for designing bridge pile protection measures. By utilizing piles with a 45-degree angle and a hole width of 0.43 from the pile diameter, the study offers insights into minimizing scour depth and enhancing the stability of bridge foundations in similar scenarios (Elnikhely, 2017).

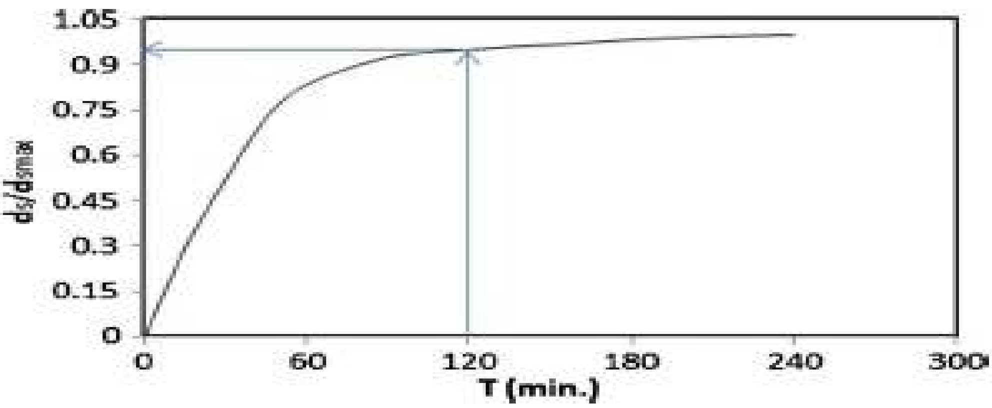

Figure 2.7 Association Amid Time and The Maximum d_s/d_s in The Absence of a Hole.

The primary objective of this research project was to examine scrubbing analysis for a bond on the Kabul River near Peshawar, Pakistan. The researchers compared the consequences of the new analysis with those obtained from the Hydraulic Engineering Center River Analysis Simulation (HEC-RAS) modeling. Figure 2–8 displays data from a typical cross-section that was input into the HEC-RAS software. Though the real form of the dock was round, the study also conducted a comparative analysis between square and circular pier. The researchers gathered demonstrating data usage of a geographic information system (Arc GIS) and then inputted it into a hydraulic modeling request. The experimental analysis involved conducting ten separate tests with varying releases and flow nadirs. The consequences of hydraulic demonstrating were compared with measurements of upstream scour depth. According to the research findings, square piers resulted in deeper scouring of the soil compared to round piers. Despite having different shapes, the scour holes displayed similar patterns. The contrast of new data revealed that the hydraulic software (HEC-RAS) made somewhat superior scrub depth measurements below similar conditions. Though, this difference reduced as the release increased (Mohammadi Givshad, Ramezani, & Khozeymehnezhad, 2020). The study's results provide valuable insights into the scouring patterns around different pier shapes and highlight the importance of hydraulic modeling software for assessing bridge foundation stability and scouring risks.

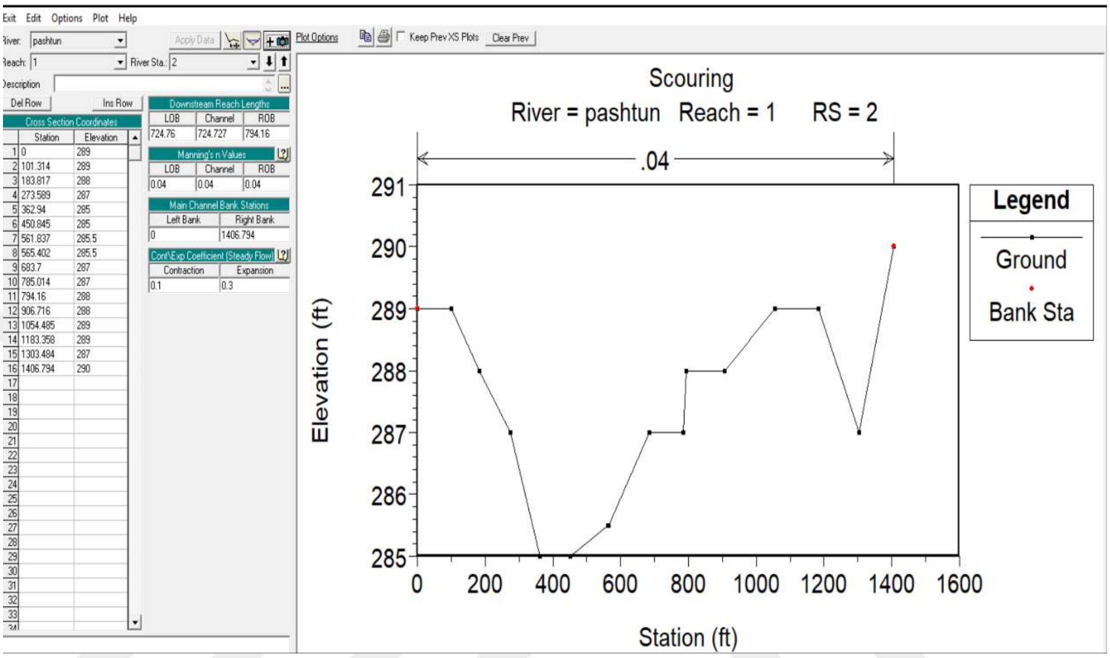

Figure 2.8 Typical Cross-Section Data Inserted in HEC-RAS.

The Batang Kalu River bridge structure has been the subject of a case study on toe scour Study Toe Scour Investigation at Batang Kalu River Bridge, The study focused on the Batang Kalu River bridge structure and conducted a case study on toe scour. To improve the accuracy of flood release project calculations, the researchers used the Kendang Empat Station. They employed arithmetical demonstrating with HEC-RAS and scour forecast by empirical reckonings to forestall the complexity of scrub on support. The simulation findings closely matched the actual scour depth observed, with an average of 2.731 meters compared to 2.83 meters. The study suggested that the increased river steepness might have influenced the local scouring around the bridge structure (Neill, 1978).

another: Study Stability Simulation of Sardar Bridge on Tapi River, In this study, the researchers focused on the "Sardar Bridge" located on the Tapi River in the study area. They used a hydraulic model to simulate the bridge's stability. The researchers evaluated scrub outlines for numerous flood incidences at various docks and supports to estimate the depth of scrub based on flow velocity. The study emphasized the importance of evaluating scour depth during the bridge's design phase to significantly reduce construction costs. Their findings recommended planning a new bridge on the upstream side of the existing bridge to ensure its hydraulic stability (Mehta and Yadav, 2020). Additionally, Figure (2-9) shows a collapsed bridge in Mahad, India, as reported by the Times of India.

Figure 2.9 Collapsed Bridge, Mahad. Source: Times of India /bridge-collapse-on-goa/liveblog.

This study conducted laboratory testing to investigate scour around bridge piers, and it also examined real-life scenarios. Diagram (2-10) shows the scour and dunes around a rectangular pier's rounded snout. The researchers aimed to determine how discharge, bed soil size, and pier distance influence the depth of scrub. They tested the scrub act about a solitary four-sided dock with a round nose below various circumstances. The results indicated that decreasing the size of the soil bed physical and cumulative movement velocity enhanced the maximum depth of scour around the pier. The shape factor (L/D), where L represents the length of the pier's four-sided portion and D denotes the diameter of its rounded nose, had a significant impact on the scour depth. The findings revealed that a shape factor of 4 resulted in a greater maximum depth of scour around the pier, with percentages of 9.7% and 50% compared to shape factors of 2.666 and 5.333, respectively.

To model the laboratory research, the researchers used a Computational Fluid Dynamics (CFD) program, specifically Flow-3D, and compared the consequences to the laboratory data. Although the simulation program generated fewer results than the experiment, it still provided valuable insights and contributed to understanding the scour phenomenon around bridge piers (Latif, 2020).

Figure 2.10 Around The Rectangular Pier Rounded Snout is Scour and Dunes.

Indeed, as described in previous summaries, various studies have addressed scour around bridge piers from different perspectives. Some of these studies have focused on developing empirical equations that establish relationships between various factors to determine the extent of scour. These equations serve as tools to predict and quantify scour depth around bridge piers under specific conditions. Additionally, researchers have explored innovative methods and countermeasures to reduce scouring effects, aiming to enhance bridge foundation stability and safety. On the other hand, some studies have conducted comparisons between the results obtained from the Hydraulic Engineering Center River Analysis Simulation (HEC-RAS) program and those derived from experimental equations. By evaluating the accuracy and reliability of HEC-RAS outputs in predicting scour, researchers can validate the software's effectiveness as a tool for assessing scour depth and its potential impacts on bridge structures. Moreover, some investigations have undertaken comparisons between the HEC-RAS program's results and the actual scour observed around certain bridges. These studies involve field data collection and measurements of scour depth in real-life scenarios, allowing researchers to assess how well the HEC-RAS program simulates and represents the scouring phenomenon in practical situations.

Overall, the combination of empirical equations, experimental data, and hydraulic modeling through programs like HEC-RAS offers a comprehensive approach to studying scour around bridge piers, aiding in the development of effective strategies to mitigate scour-related risks and optimize bridge design and construction.

This research aims to conduct practical experiments to simulate the scour results of bridge supports. A comparison will be made between the scour values obtained from the practical experiments and the results generated by the Hydraulic Engineering Center River Analysis Simulation (HEC-RAS) program. This approach sets this research apart from many previous studies that have not undertaken such a comparison. The study will specifically focus on single circular supports and rectangular supports with semi-circular ends, considering various diameters, discharge rates, and types of soil. By conducting practical experiments and comparing them with HEC-RAS results, the research seeks to gain a comprehensive understanding of scour behavior around different support structures under varying conditions. This comparative analysis will provide valuable insights into the accuracy and reliability of the HEC-RAS program in predicting scour depth, as well as the influence of different factors on scour development around bridge supports. The research outcomes can contribute to the advancement of bridge design and construction practices, enabling engineers to make more informed decisions regarding scour mitigation measures and bridge foundation stability.

CHAPTER 3

NUMERICAL MODELING

3.1 Introduction to HEC-RAS

The U.S. Army Corps of Engineers created the computer program HEC-RAS. The usual step approach for computing the water surface profiles is included in this application. HEC-RAS, the Hydrologic Engineering Center's River Analysis System, is a complete software program designed for multitasking and interactive use. Engineers from all around the world have long utilized the HEC-RAS program, which was established and developed by the Army Engineering Office of the United States. Scour simulations were made possible in the 2006 (HEC-RAS) program. Grids, channels, branches, or individual rivers can all be properly modeled using the HEC-RAS model. This software's features can be utilized to evaluate both steady and erratic flows, sub-critical and supercritical flows, culvert design, sediment transport simulation, and other problems.

The software also establishes the scour depth of bridge piers built on rivers utilizing the hydraulic flow data, the geometry and geometric features of the bridge pier, and the material and shape of the substrate surrounding the river. HEC-RAS is a comprehensive software system designed for interactive use in a setting where multiple tasks are being performed at once.

A graphical user interface (GUI), data storage and administration capabilities, independent analysis components, visuals, and reporting tools are all parts of the system. Along with the components for river analysis, the system also features a number of hydraulic design elements that may be applied after computing the water surface profiles.

3.2 Limitations of the experiments that were simulated in the (HEC-RES) program

3.2.1 Determinants of Practical Experiments by Researcher (Ahmed Ashur)

The laboratory experiments for this study were done in the fluid laboratory of the Department of Civil Engineering at the University of Anbar, by measuring the depth of the Scour around the Piers. All experiments were carried out under clear water conditions.

3.2.1.1 Laboratory Channel and Accessories

The hydraulic channel used in lab tests is an open channel made of iron that has a thickness of 4 mm for the basins and the walls of the channel are made of transparent glass with a thickness of 10 mm. The canal is 18.7 meters long in total, with the top basin measuring 3.7 meters and the lower basin at 3 meters in length and 0.77 meters in height, its upper level is the same as the upper basin's base level. Three filters in the lower basin help to calm the runoff water as it enters the 12 m long, 0.5 m wide, and 0.5 m high canal. The water flowing through this closed system channel, which has a lower base that can alter its inclination, returns to the ground tank or feeding basin, which has dimensions of (7.5 * 2.5 * 1.2) meters. Using a pipe with a 5-inch diameter and a valve to manage the pump's design discharge of 135 liters/second, the channel is filled with runoff from the feeding trough. An illustration of the components of the open laboratory channel used for experiments is shown in Figure (3-1).

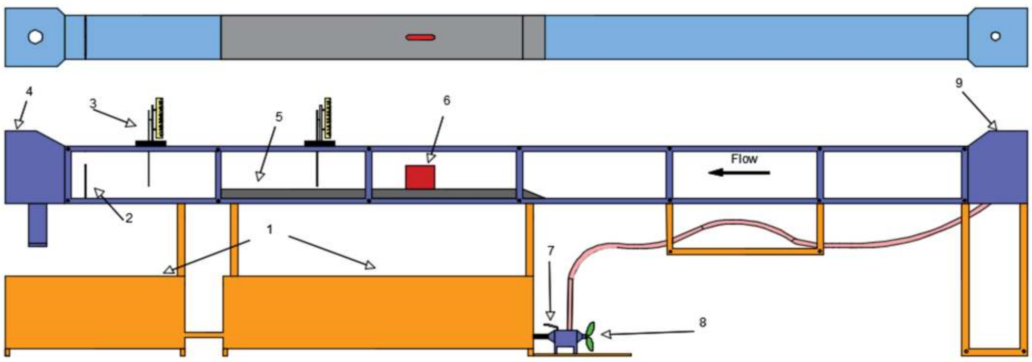

(1) Water tanks (2) Weir (3) Point gauge (4) D/S reservoir (5) Soil bed (6) Pier (7) Valve (8) Pump (9) U/S reservoir

Figure 3.1 Scheme of the Channel was Used in Laboratory Experiments.

The research area, which is in the center of the channel and is 3 m long and 10 cm deep, contains the sand layer that was utilized in the tests. To allow water to drain through it after each experiment, its end was constructed as a porous barrier. Use for Measure the bottom levels, the depth of the Scour surrounding the abutments, the size, and the shape of the Scour hole using a point scale (Point Gage) with a precision of 0.001 m. And fixed gate to regulate the amount of run-off depth of discharge needed for each experiment is located at the end of the channel.

3.2.1.2 Laboratory Piers Models

In this research, three models of cylindrical supports (25, 32, and 50 mm) in diameter as well as rectangular supports with semi-circular ends manufactured of wrought iron and painted with oil-based dyes were utilized in the studies. These experiments were conducted:

- ❖ Three discharges were passed in nine experiments on single cylindrical supports with varied diameters (25,32,50) mm.
- ❖ 27 trials were conducted in which the Scour was evaluated around three distinct, succeeding pillars (25, 32, 50) mm, with the distance between each pillar being altered three times (2D, 3D, 4D), and three different discharges being passed in each case.
- ❖ Nine experiments were carried out on rectangular pillars with semicircular ends that were (25, 32, 50) mm in diameter and totaled (7D, 9D, 11D) mm in length, i.e., the length of the pillars is the same as the distance between the first and last pillars of three successive pillars.

3.2.1.3 Soil Used in The Experiment

In order to conduct experiments on the canal, river sand was employed as the bottom material with a length of 3 m and a thickness of 10 m in the study region. The sieve analysis was performed as indicated in Figure (3-2), with the values of some determinants related to its specifications that are employed in the experiments calculated and given in Table (3-1) to determine the features and specifications of this soil.

Table 3.1 Some specifications of river sand used in the study

Values	Variables
0.3 mm	Average diameters of sand grains(d_{50})
1.45	The geometric standard deviation of the granules(σ_g)

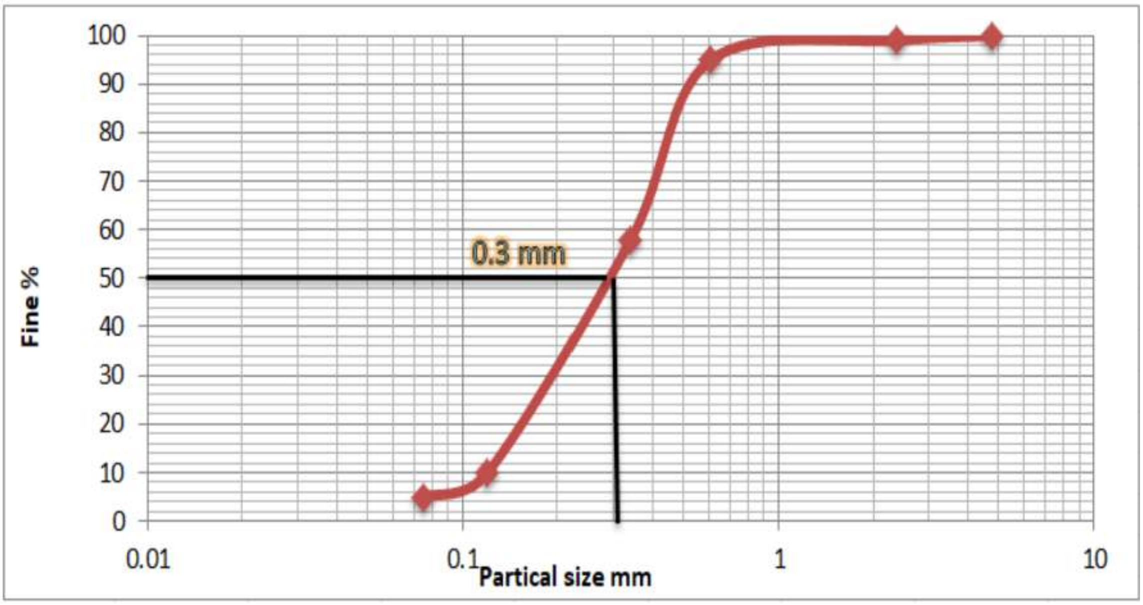

Figure 3.2. Size Distribution of The Soil Particles Used in The Study.

The distribution of sand grains employed in this study is irregular because, according to the researcher (B. W. Melville & Coleman, 2000) Sand is considered regular when its standard deviation (σ_g) value is less than 1.3.

3.2.1.4 Determinants of Hydraulic Experiments

Three discharges were utilized for each model of the Piers, and the three flow depths are shown in Tables (3–2) together with the speed employed, the Froud number, and the value of the critical speed (V_c) needed to initiate the movement of the bottom materials.

Table3.2 Determinants of hydraulic experiments

Discharge Q (l/sec)	Flow depth Y (M)	Area A (M^2)	Velocity rate V (M/Sec)	Critical velocity Vc (M/Sec)	Flow intensity V/Vc	Froude number Fr
20	0.28	0.14	0.142857	0.253886	0.562682	0.08619
30	0.31	0.155	0.193548	0.25823	0.74952	0.11099
40	0.35	0.175	0.228571	0.263506	0.867423	0.1234

3.3 Set-Up of The Numerical Model

Using HEC-RAS, there are five key processes to create a hydraulic model: beginning a new project, entering geometric information, entering flow information, entering boundary conditions, carrying out the hydraulic computations, and viewing and printing of the outcomes.

3.3.1 Beginning a New Project

In order to create a hydraulic model using HEC-RAS, you must first choose the directory you wish to work in, then give your new project a title. Open the main HEC-RAS window's File menu and choose "New Project" to start a new project. By doing this, the window of "New Project" will open as seen in (Figure (3-3).

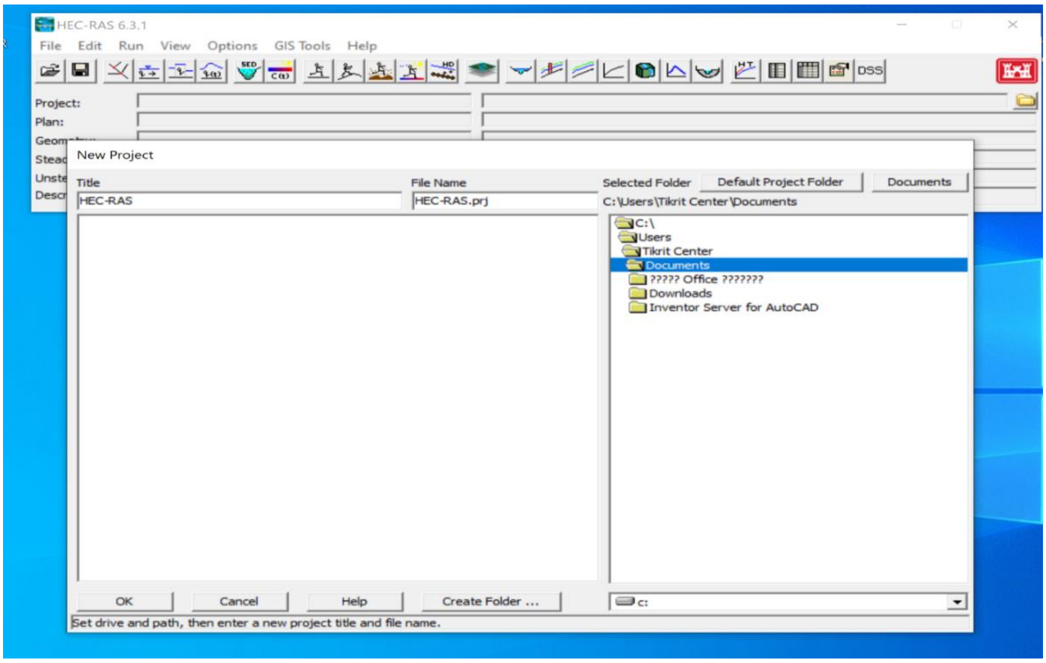

Figure 3.3 Window of a New Project.

As seen in Figure (3-3), you should first choose the drive and path that they should use before entering the project title and file name. To choose a path, double-click the desired directory in the directory box. The user is not permitted to alter the project filename's required "prj" extension. When you have finished entering all the necessary information, click "OK" to confirm that it has been accepted. The project title and the location where the project will be stored will appear in a message box when the OK button has been clicked. Click the "OK" button to confirm that the information is accurate. Clicking the Cancel button will return you to the New Project window if the information is incorrect. Before entering either Geometric data or Flow data, the user needs to decide whether they want to operate in US Customary or Metric units. This procedure is completed by choosing Unit System in the main HEC- RAS window's "Options" menu.

3.3.2 Entering Geometric Data

The necessary geometric data must next be entered, which comprises a background map layer (Optional), cross-section data, stream system connectivity data (River System Schematic), and structural hydraulic data (bridges, culverts, weirs, etc.). On the main window of HEC-RAS, geometric data can be entered by choosing “Geometric Data” from the “Edit” menu. When you select this option, the geometric data window depicted in Figure (3-2) will appear (although yours will be blank the first time you bring up this screen for a new project). The user must choose whether or not to georeferenced their model before entering any geometric data. Prior to creating the geometric data in the HEC-RAS, the modeler must first incorporate the schematic of the river system. This is done reach-by-reach (in the positive flow direction) by pressing "River" and a "Reach" button, then drag in a reach from upstream to downstream. After drawing the reach, the user is required to enter "River" and "Reach" identification.

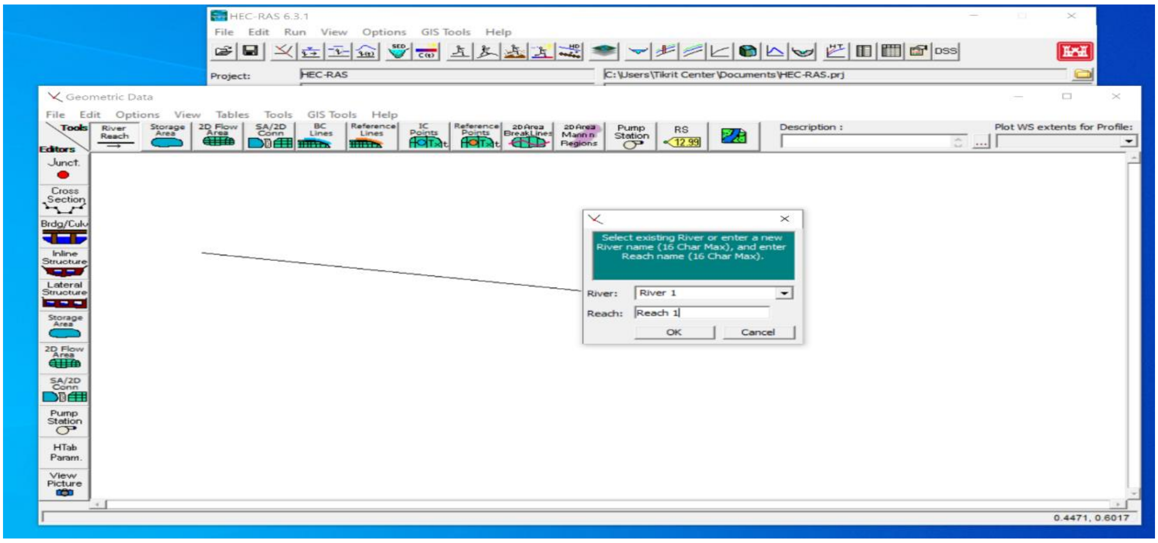

Figure 3.4 Geometric Data window.

The user can begin entering cross-section and structural hydraulic data once the river system's schematic is developed (See Figure 3-2). The "River", "Reach", and "River Station" identifiers identify the cross-section's location within the river system. The "River Station" identification needs only be a numeric value rather than the precise river station (in kilometers or miles) where the cross-section is situated on the stream (e.g., 1.1, 2, 3.5, etc.). The editor of cross-section data illustrated in Figure (3-5) displays the fundamental information needed for each cross-section. Any cross-section requires the following information, among others: the cross-section point coordinates, the downstream reach lengths (the distance from one cross-section to the next downstream), and Manning's values (n) are all required, with the left overbank, main channel and the right overbank Manning's n values being the absolute minimum. Manning's values (n) are variable both vertically and horizontally; the main channel bank stations (which specify the right and left banks' limits of the main channel); and coefficients of contraction and expansion are further variables (whose default values are 0.1 and 0.3, respectively). After completing the "River Station", we enter the cross-section data see Figure (3-5). Then, as shown in Figure (3-6), which illustrates the addition of the channel cross sections, we enter the specified channel's cross sections at certain points along the channel or, if the channel is equal, we copy the cross section at those points.

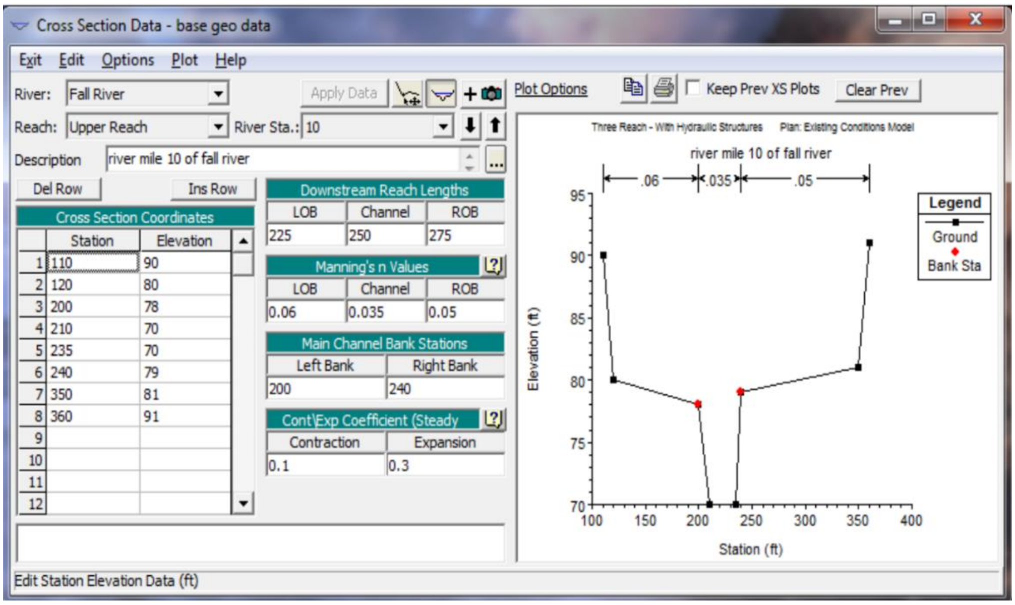

Figure 3.5 Cross-Section Data Editor.

After completing the addition of the cross-section information, we enter the location and data of the hydraulic structure as shown in the figure (3-6).

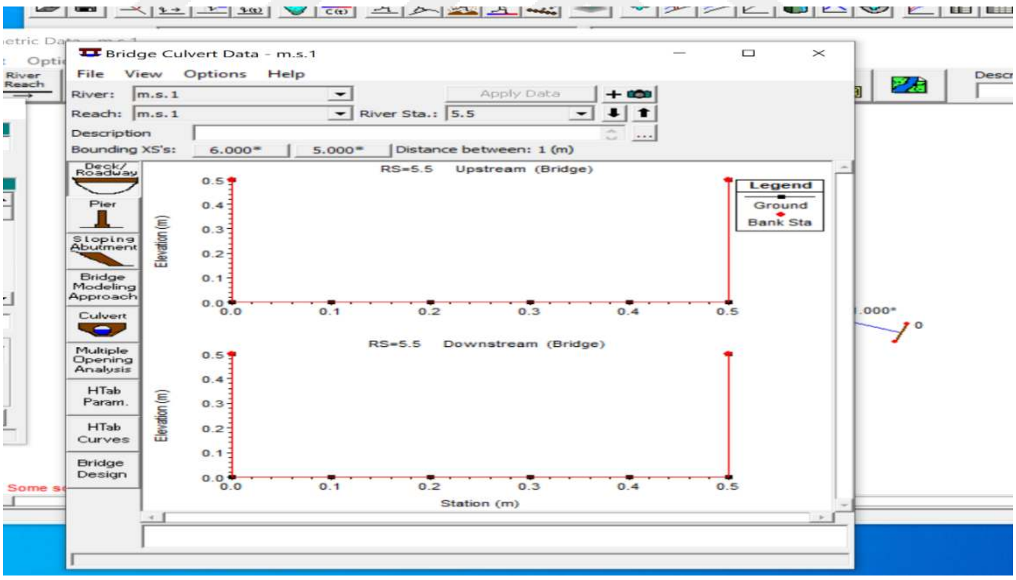

Figure 3.6 Location and data of the hydraulic structure.

3.3.3 Entering Flow Data and Boundary Conditions

After entering the geometric data, the modeler can then enter data for either steady flow or unstable flow. Depending on the type of studies that will be conducted, as for our studies, fixed flow and disagreement expenses are approved, and different types of flow data must be entered. Figure (3-7) showing the editor of the steady flow data serves as an illustration of the steady flow data entering form. The number of profiles that need to be computed, the flow information, and the river system’s boundary conditions make up steady flow data, as illustrated in Figure (3-7). Every reach in the system requires the entry of at least one flow. In addition, the river system's flow can be modified anywhere. All profiles need the entry of flow values. The computations need boundary conditions to be completed. To do a subcritical flow analysis, only the downstream boundary conditions are needed. A supercritical flow analysis only requires the upstream boundary conditions. Both the downstream and the upstream boundary conditions are necessary if the modeler wants to do the calculation of a mixed flow regime. The “Boundary Conditions” data entry form is opened by clicking the “Reach Boundary Conditions” button on the entry form of the steady flow data. After entering all the steady flow information and the boundary conditions, the modeler must save this data to the hard drive of the machine. To achieve this, use the “File” menu option found on the menu bar of “Steady Flow Data” and select Save Flow Data As. The filename is automatically assigned; just the flow data's title needs to be provided.

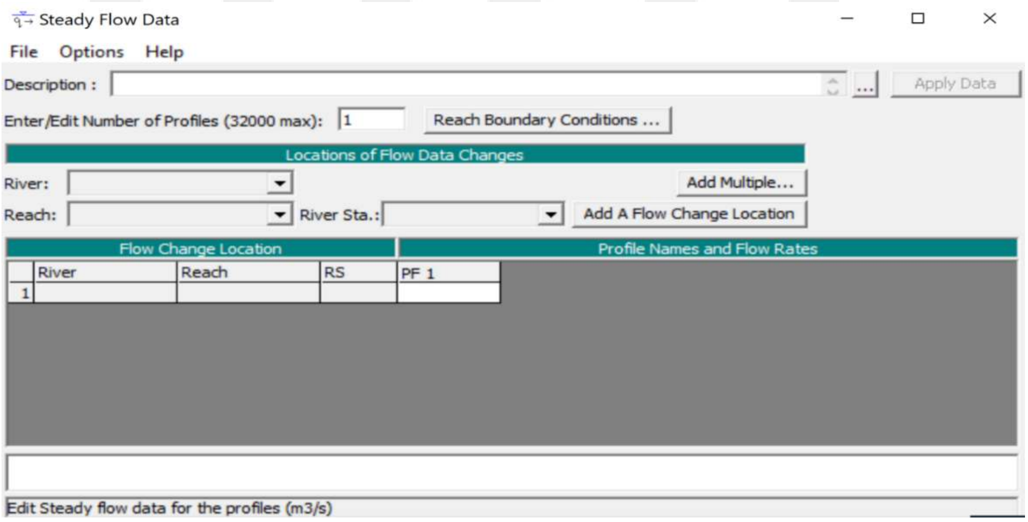

Figure 3.7 Window of Steady Flow Data.

3.3.4 Performing the Hydraulic Computations

After entering all of the geometry and flow information, the modeler will be able to start doing the hydraulic computations. The HEC-RAS supports five different computing types: sediment transport/mobile boundary modeling, unsteady flow analysis, steady flow analysis, hydraulic design functions, and water quality analyses. Figure (3-8) illustrates how the modeler constructs a “Plan” by choosing a particular collection of flow data and geometric data. The "Steady Flow Analysis" window allows for the creation of a plan by selecting "Create Plan" from the File menu option. A flow regime can be chosen for which calculations will be made by the model when a title and a short identifier (Short ID) for a plan have been input. Calculations for the supercritical, subcritical, or mixed flow regimes are offered. Additional features that can be accessed through the "Options" menu include doing an analysis of floodway encroachment, conveyance calculation options, setting regions for calculating the output of the flow distribution, calculation tolerances, methods of friction slope, critical depth computation method, critical depth output, data checking, split flow optimization, viewing the log file output and setting log file levels. The steady flow calculations can be carried out by hitting the "Compute" button at the bottom of the steady flow analysis window once the modeler has chosen a plan and configured all the options of calculation. By pressing this button, the HEC-RAS system compiles all the data related to the selected plan and publishes it as a run file. Once the system has been provided the name of the run file, the steady flow model is then done. This procedure is carried out in a different window. As a result, while the modeler is running, other jobs can be completed (Akilli, Sahin, & Tumen, 2005).

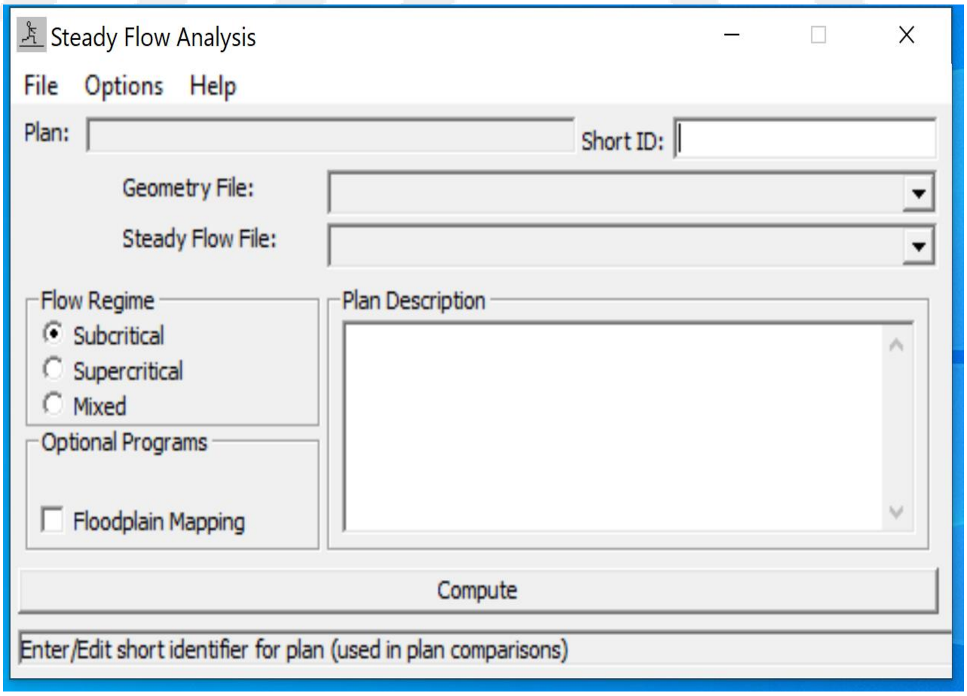

Figure 3.8 Steady Flow Analysis window.

3.3.5 Entering Pier Scour Data

Either the Froehlich (1988) equation or the Colorado State University (CSU) equation can be employed to calculate the pier scour (Richardson et al., 1990). In this study, the program's default equation, the CSU equation, is used. As illustrated in Figure (3-9), you only need to enter the following: the pier's nose shape (K1), the bed state (K3), the angle of attack for the flow hitting the piers, and a D95 size fraction for the bed material. The HEC-RAS output file is automatically used to calculate all other values. The user can choose to calculate the pier scour using either the maximum velocity and depth in the main channel or the depth and the local velocity at each of the piers, as shown in Figure (3-9). In general, the main channel thalweg potential to move back and forth within the opening of the bridge is taken into account by using the maximum velocity and depth. The highest potential scour could happen at any one of the bridge piers as a result of the main channel thalweg migration.

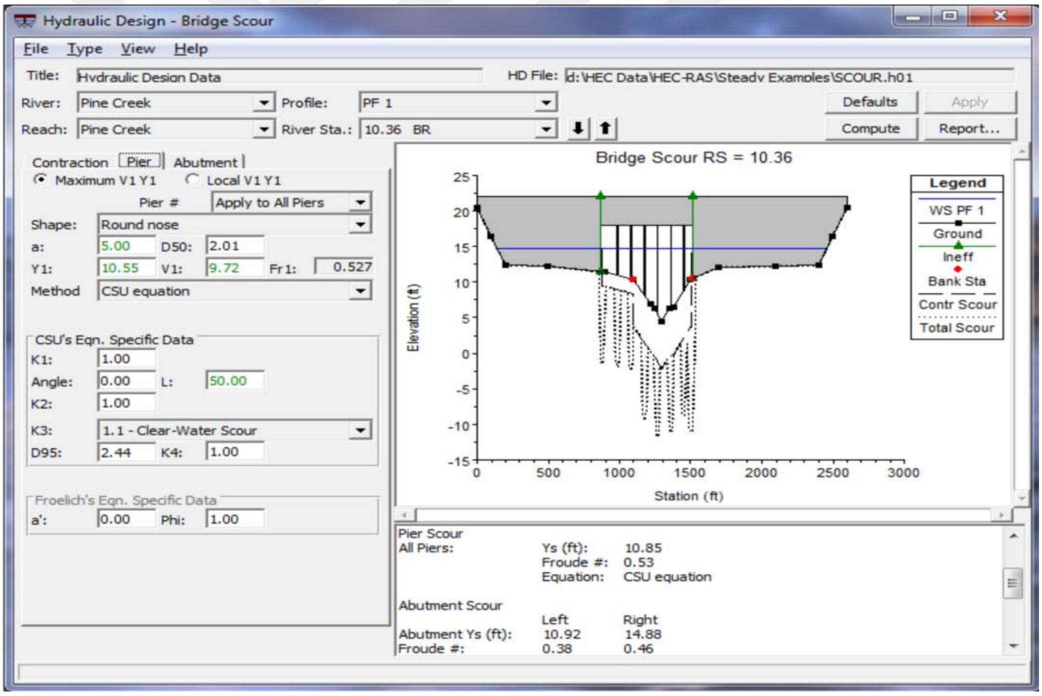

Figure 3.9 Entering Pier Scour.

3.3.6 Viewing and Printing Results

The modeler will be able to start viewing the outcomes after completing all the calculations. Many output features can be accessed through the main window's View option. These options consist of water surface profile plots, cross-section plots, general profile plots, X-Y-Z perspective plots, rating curve plots, hydrograph plots, and hydraulic property tables (if the simulation of an unsteady flow was done), detailed output tables, profile summary tables, and summaries of errors, notes, and warnings. Figure (3-10) depicts a cross-section plot as an example. It is possible to plot the cross-section via just choosing the proper “River”, “Reach”, and “River Station” from the list boxes found at the plot’s top. The up and down arrow buttons allow the user to navigate the plots. The cross-section plot's Options menu offers a number of plotting options. These options comprise zoom in and zoom out, pan, full plot, and animate, as well as options for lines, symbols, labels, scaling, and grids. You can also choose which plans, profiles, and variables to display (Azizian, AmirTakoldani, & GholiZadeh, 2010).

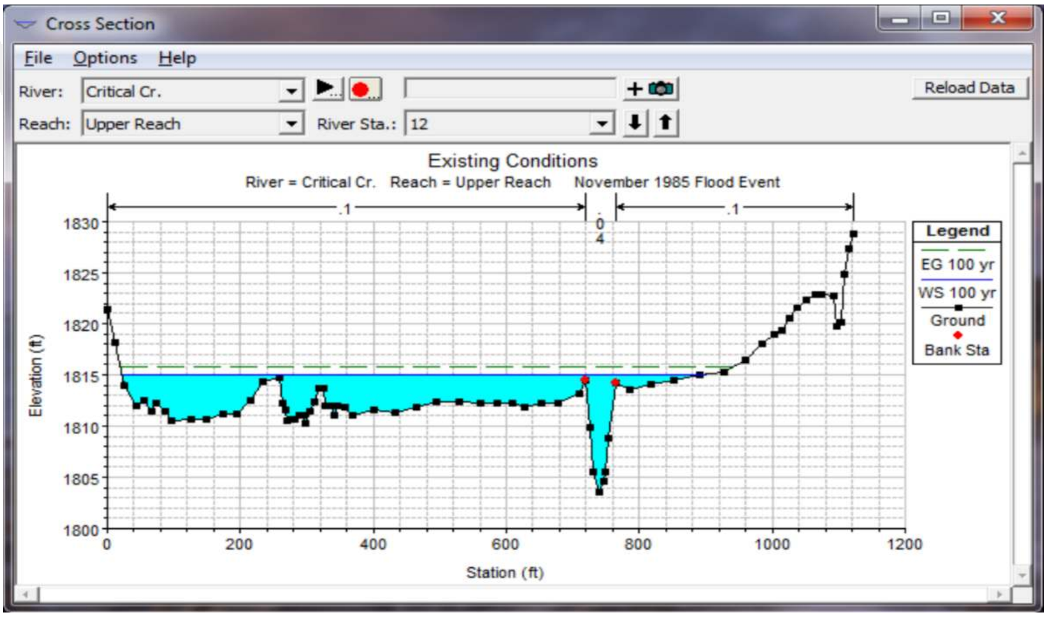

Figure 3.10 Cross Section Plot.

The visuals can be produced in hard copies in two different methods. The user's chosen printer or plotter can get graphic plots straight from HEC-RAS using the Windows Print Manager. Moreover, graphic plots can be copied to the Windows clipboard. Once the plot has been copied to the clipboard, it is then possible to paste it into other applications, like the word processor. On the various plot windows, the File menu offers both of these choices. The profile plot offers each option that is present in the cross-section plot. When modeling a river system with several reaches, the user can also choose which specific reaches to plot. The tabular output is offered in two types. In the first type of tabular output (Detailed Output Table), individual cross-section hydraulic results are provided in detail. Few hydraulic variables are displayed for numerous cross-sections and multiple profiles in the second form of tabular output (Abdallah Mohamed & Abdel-Aal).

3.3.7 Testing Program

In this study, forty-five models were used, each with a drawing and data entry for a single evaluation. The data entered for one model is shown in Figure (3-11). The simulation output of the model is then displayed to us along with a thorough representation of the Scouring borders surrounding the column. The outcomes of one of the trials are shown in Figure (3-11).

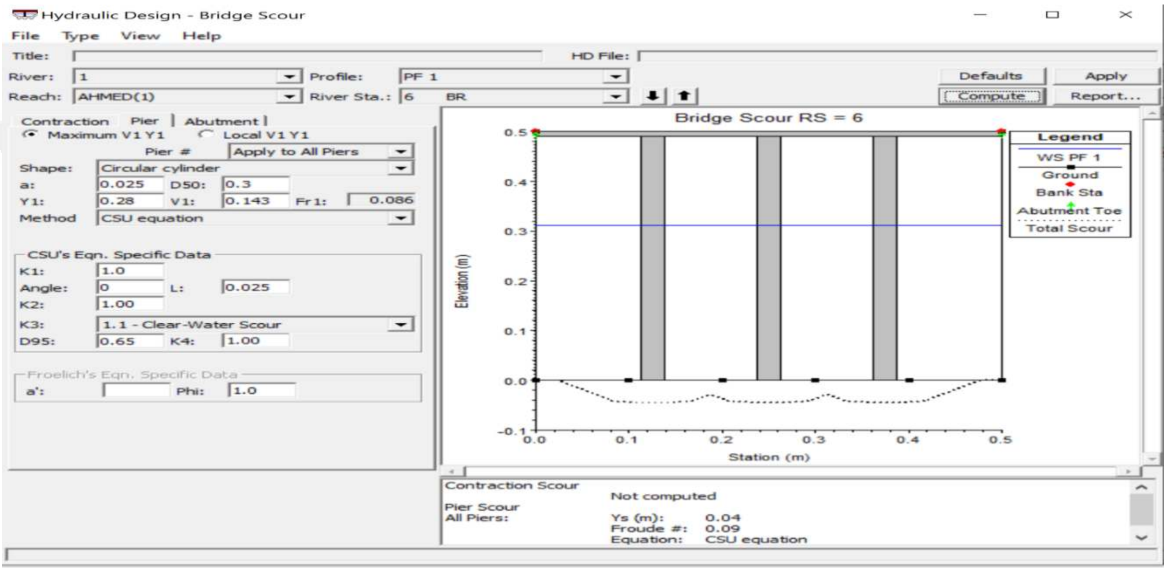

Figure 3.11 The outcomes of one trial.

3.4 Correction Factor For Angle of Attack of The Flow On The Pier (k$_2$)

The correction factor for the angle of attack of the flow on the pier (K2) was chosen by simulating six variable values of the angle of attack of the flow (K2). The results of the experiments for the values in the equation Nash–Sutcliffe efficiency coefficient (NS) The NS values lie between (−∞ and 1). A range between 0.5 and 1 is acceptable, while the best value of NSE is one. The NS coefficient is determined from Eq. (4) (Moriasi et al., 2007).

$$NSE = 1- \Sigma t\,(O - S)2 \,/\, \Sigma t\,(O - \bar{O})2 \quad (3\text{-}1)$$

Where:

O =is the observed variable.

S= is the simulated variable.

Ō =is the time average of the observed variable.

The value of the correction factor for the angle of attack of the flow (0.6) was as close as possible to the practical experiments, and it was adopted in this study. As shown in figure (3-12), the value of NSE (0.77) was the closest thing to practical experiments.

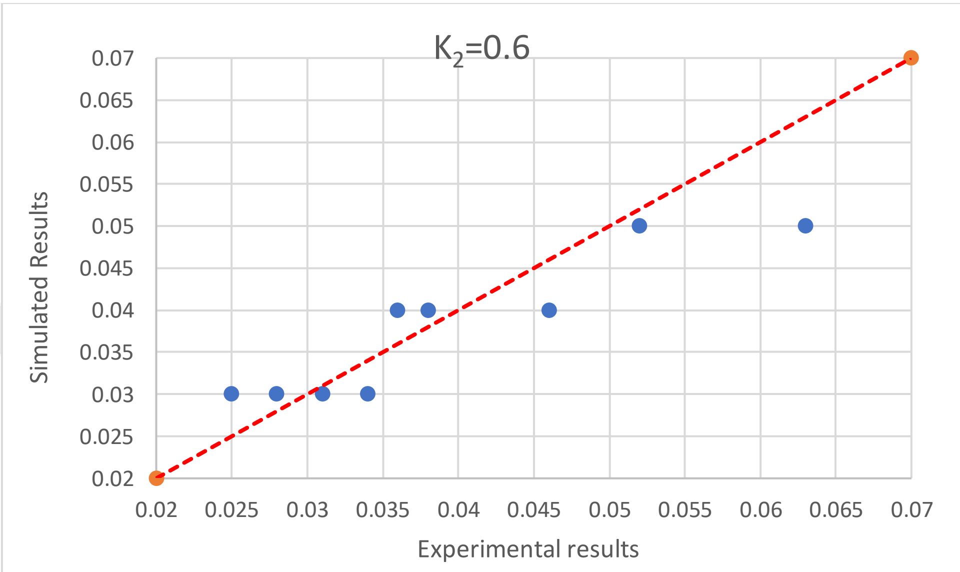

Figure 2.12 Shows the results of the simulation process and its closeness to practical experiments (NSE=0.77).

As for the rest values of the correction factor for the angle of attack (0.5,0.65,0.7,0.75 and 1), the values of NSE were far from practical experiments, as shown in the figures, from Figure (3-13) to Figure (3-17), respectively, for each value of the friction values.

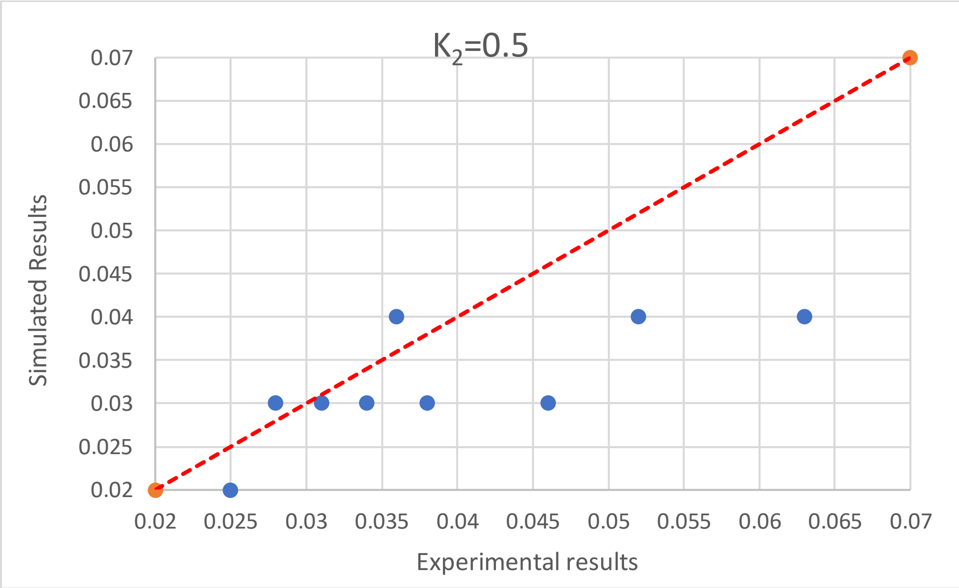

Figure 3.13 Shows the results of the simulation process and its closeness to practical experiments (NSE=0.22).

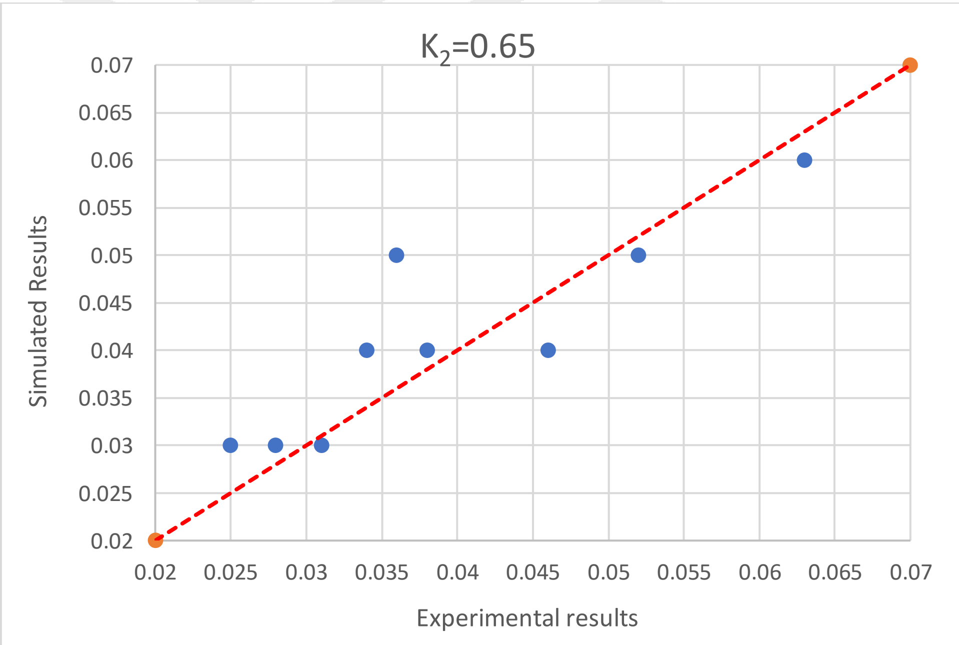

Figure 3.14 Shows the results of the simulation process and its closeness to practical experiments (NSE=0.74).

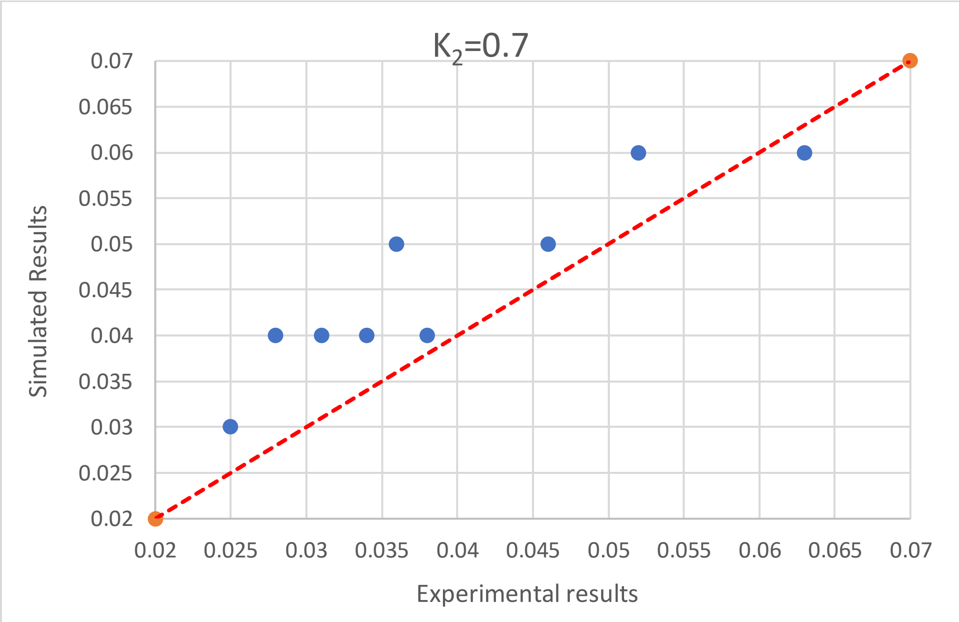

Figure 3.15 Shows the results of the simulation process and its closeness to practical experiments (NSE=0.63).

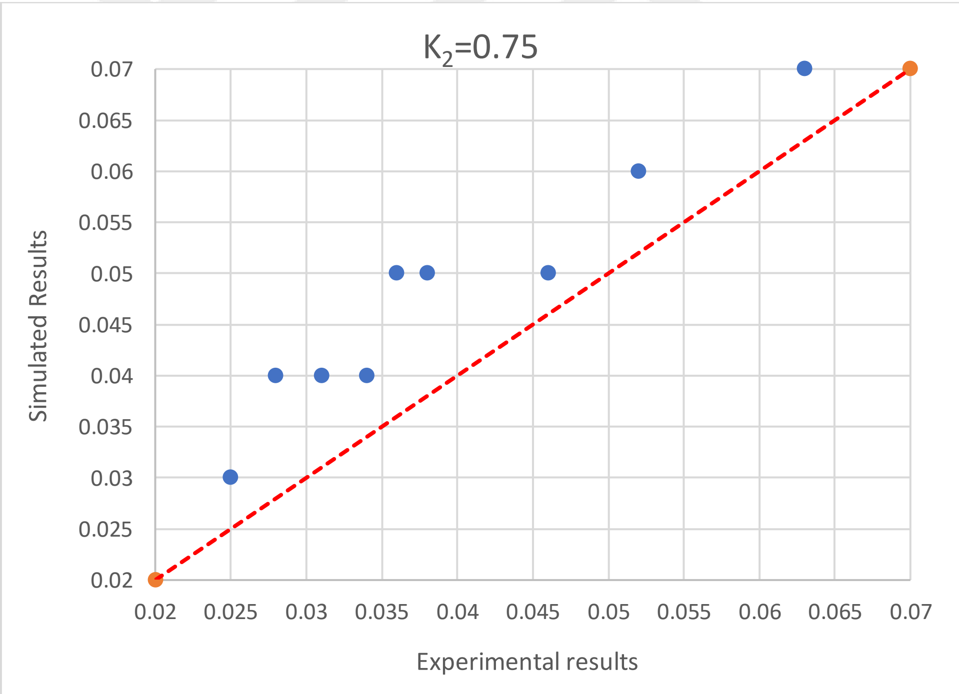

Figure 3.16 Shows the results of the simulation process and its closeness to practical experiments (NSE=0.59).

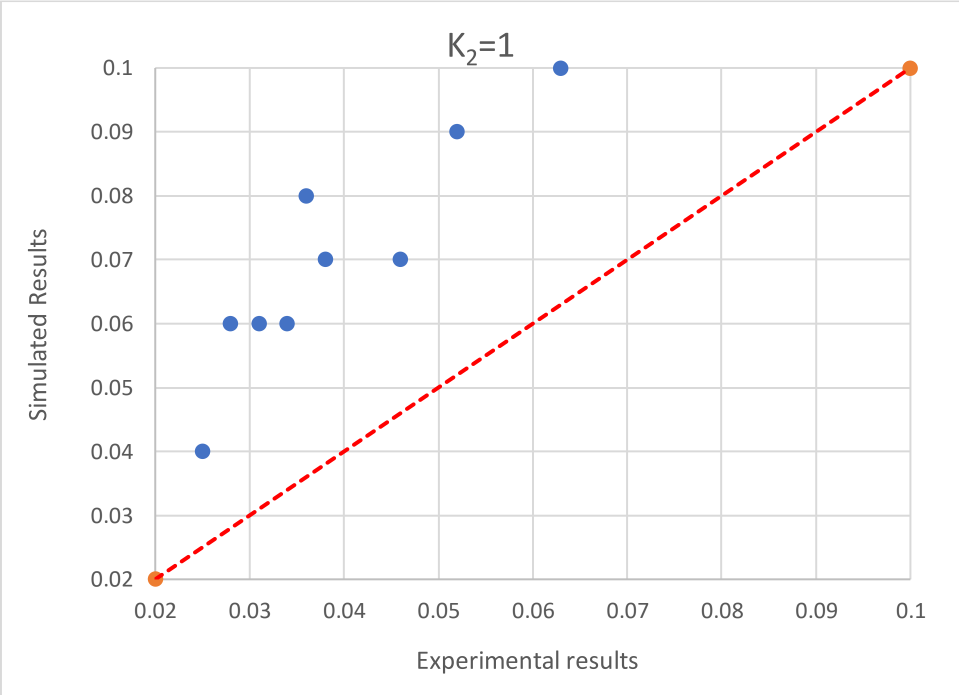

Figure 3.17 Shows the results of the simulation process and its closeness to practical experiments (NSE=0.63).

3.5 Dimensional Analysis

In order to determine the size of the effect, discover the joint effect, determine the cause of the discrepancy (when the results differ between studies), or arrive at a unified conclusion with greater statistical power, Dimensional -analysis is a statistical procedure that involves gathering data from multiple quantitative studies in an organized and systematic manner. According to the dimensional analysis theory, the depth of the scour (ds) will depend on the other variables in the following way:

$ds=f(D, \rho, g, d50, \mu, V, y, B, S, S_H)$ ……………………………………….. (3-2)

ds= depth of the scour

d50= median particle size of soil.

g= gravitational acceleration.

V= velocity of water.

y= depth of water from the surface of bed soil material to the surface of water.

D = Roller pier diameter.

B = channel width.

S = Distance between piers Consecutive.

SH= Distance between piers contiguous.

ρ = The mass density of water.

μ = Dynamic viscosity of water.

$f_1(ds, D, \rho, g, \mu, d50, V, y, B, S, S_H) = 0$ ……………………………………..(3-3)

In addition, adopting the variables density (ρ), velocity (V), distance between piers contiguous (SH), and depth (y) according to Buckingham's theory. The basic recurring equation is as follows:

$f_2(\pi_1, \pi_2, \pi_3, \pi_4, \pi_5, \pi_6, \pi_7) = 0$ ……………………………………………(3-4)

Representing:

$\pi_1 = \rho^{a1} V^{b1} y^{c1} ds$

$\pi_2 = \rho^{a2} V^{b2} y^{c2} B$

$\pi_3 = \rho^{a3} V^{b3} y^{c3} \mu$

$\pi_4 = \rho^{a4} V^{b4} y^{c4} g$

$\pi_5 = \rho^{a5} V^{b5} y^{c5} D$

$\pi_6 = \rho^{a6} V^{b6} y^{c6} S$

$\pi_7 = \rho^{a7} V^{b7} y^{c7} d50$

By conducting a dimensional analysis of (π_1):

$\pi_1 = \rho^{a1} V^{b1} y^{c1} ds$

$M^0 L^0 T^0 = (ML^{-3})^{a1} (LT^{-1})^{b1} (L)^{c1} (L)^1$

For M: $a_1 = 0$

For T: $b_1 = 0$

For L: $c_1 = -1$

$\pi_1 = \frac{d_s}{y}$, by the same way:

$\pi_2 = B/ y$, $\pi_3 = y\ g\ /V^2 = Fr$, $\pi_4 = \mu\ /\rho\ V\ y = Re$, $\pi_5 = S\ /y$, $\pi_6 = D/ y$,

$\pi_7 = d50/ y$, $\pi_8 = S_H/ y$

Where:

Re: Reynolds number

Fr: Froude's number

$$f_3 = \left(\frac{d_s}{y}, \frac{B}{y}, Fr, Re, \frac{S}{y}, \frac{SH}{y}, \frac{D}{y}, \frac{d50}{y} \right) = 0 \quad \text{……………………………………….(3-5)}$$

$$\frac{d_s}{y} = f_4 \left(\frac{B}{y}, Fr, Re, \frac{S}{y}, \frac{SH}{y}, \frac{D}{y}, \frac{d50}{y} \right) \quad \text{.(3-6)}$$

And since the width of the channel (B) and the soil of the bottom material (50d) are constant for all experiments, the Reynolds number is also large. The fluid behaves according to the theory of lack of viscosity according to (Knauss, 2017), where the flow is turbulent flow, that is, the effect of viscosity is neglected. Therefore, the scouring will depend on the non-dimensional variables. as shown in the following equation:

$$\frac{d_s}{y} = f_5 \left(\frac{D}{y}, Fr, \frac{S}{y} \right) \quad \text{……………………………...…………………………. (3-7)}$$

CHAPTER 4

RESULTS AND DISCUSSIONS

4.1 Introduction

In this chapter, the laboratory results from researcher Ahmed Ashour for both single and group Piers will be studied, analyzed, and compared. and compared with the same experiments and variables using simulation by the program (HEC-RAS) For the researcher. and understanding the mechanism of the scouring process around the stents in all of the studied cases as well as the influence of the dependent variables on the depth of the scouring, such as the stents' diameter, spacing, flow velocity, depth, and Froud number, and comparing these to the depth of the scouring. By contrasting the use of a single pillar, a series of succeeding pillars, as well as rectangular pillars with semicircular ends, the scouring mechanism will be explained. Based on the data extracted from the (HICRAS) program, a situational equation will be derived to calculate the expected depth of scouring according to the study parameters using the statistical program (SPSS).

4.2 The Mechanism of Scour

The flow becomes turbulent when a foreign body of a certain mass is present in the waterway, such as bridge abutments of all shapes. Because the water is concentrated in front of the pier when it reaches it and then immediately disperses around its sides, the flow creates a spiral motion as it approaches the front face of the pier, which is the creation of horseshoe-shaped vortices at the base of the pier due to a shift in pressure that causes a change in flow direction from the horizontal flow to the vertical downward flow. This causes some soil particles to be lifted depending on the strength of the vortex. This is seen by the formation of scour around the pier and the movement of sediment from the front to the back of the pillar. The amount of this rise is dependent on the speed of flow and the shape of the Pier, as stated by the researcher (Burrell,2023), and it results from the water's collision with the front face of the pier creating surface vortices that cause the water level to rise in front of the pier. Figure (4-1) shows the flow of water in the form of a horseshoe and on the tops of the Piers (B. Melville & Sutherland, 1988).

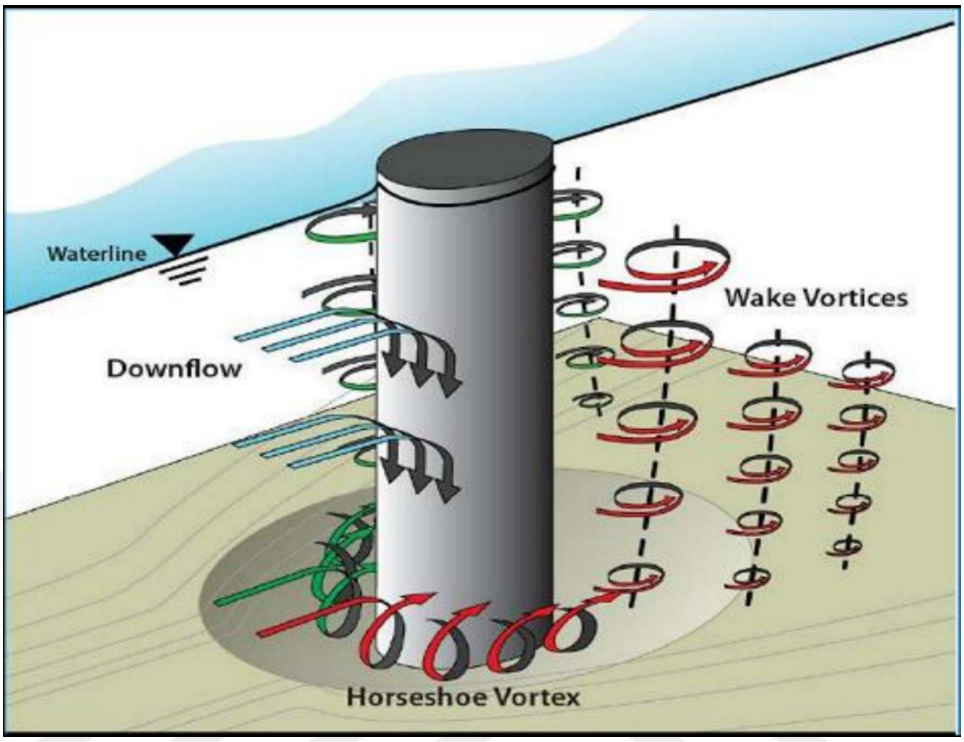

Figure 4.1 Shows the flow of water in the form of a horseshoe and on the tops of the Piers.

When water is spilled, erosion starts to occur as the grains of the bottom soil start to move as a result of creating a force that causes particles to move from the front of the support's base to the back of the support. This movement of particles gradually increases until Scour stabilizes, which happens when the erosion hole widens, weakening the power of the vortices, as stated by the researcher (B. W. Melville, 1997).

4.3 The effect of the main determinants on the depth of Scouring for cylindrical Pier

4.3.1 Effect of pier diameter and distance on the depth of scour

The depth of scouring of soil was shown to be directly and negatively impacted by increasing the diameter of the piers, as evidenced by the results of the simulation of the practical experiments displayed in the table (4-1), as the depth of scouring increases with the increase in the diameter of the individual Piers and also increases with the increase in runoff drainage. In addition, The simulation results shown in Table (4-1) that have been conducted, it was discovered that the depth of Scouring is directly correlated with the increase in the diameter of the Piers, as the Scouring around the columns increases with the pier diameter and also increases with increases the discharge.

Table 4.1 Results of scour around single cylindrical piers

Fr	Q (m^3/sec)	D (m)	V (m/sec)	y (m)	D/y	Ds $_{Hec-Ras}$ (m)	Ds/y (Hec-Ras)	Ds $_{exp.}$ (m)
0.086	0.02	25	0.143	0.28	0.089	0.03	0.107	0.025
0.111	0.03	25	0.194	0.31	0.081	0.03	0.097	0.028
0.123	0.04	25	0.229	0.35	0.071	0.03	0.086	0.034
0.086	0.02	32	0.143	0.28	0.114	0.03	0.107	0.031
0.111	0.03	32	0.194	0.31	0.103	0.04	0.129	0.038
0.123	0.04	32	0.229	0.35	0.091	0.04	0.114	0.046
0.086	0.02	50	0.143	0.28	0.179	0.04	0.143	0.036
0.111	0.03	50	0.194	0.31	0.161	0.05	0.161	0.052
0.123	0.04	50	0.229	0.35	0.143	0.05	0.143	0.063

where the highest value of scouring in (Hec-Ras) program, (50) mm, happened while utilizing a pier with a diameter of (50) mm and a discharge of (40) liters/second was applied to it. The highest value of scouring in the laboratory experiments was (63) mm while using a pavement with a diameter of (50) mm and a discharge of (40) liters/second was applied to it. Figure (4-2) shows the relationship between the depth of scouring and the diameter of the individual pier.

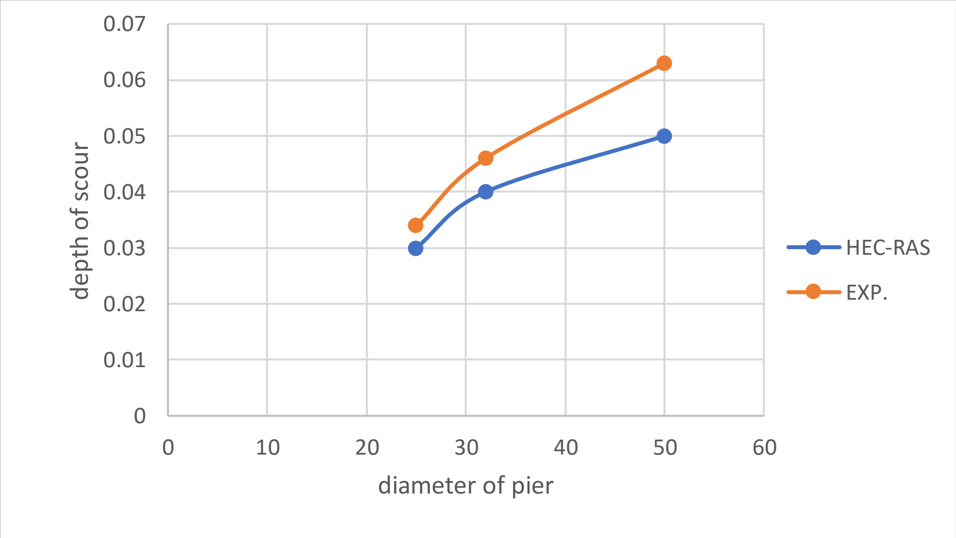

Figure 4.2 The relationship between the depth of scour and the diameter of the single cylindrical pier when (Q=40 l/sec).

Figure (4-3) and Figure (4-4) for each of the discharges (30,20) l/sec respectively show the connection between the depth of the scouring and the discharge in the channel.

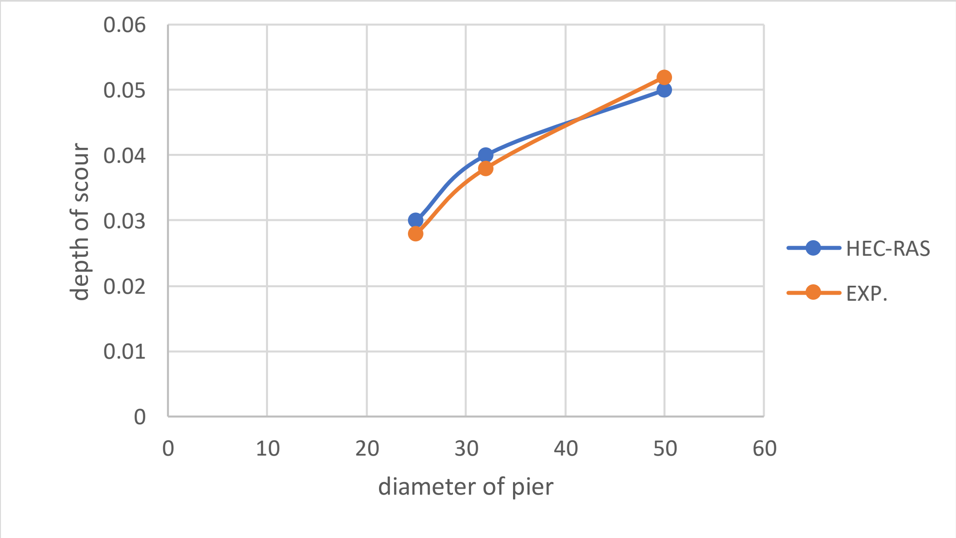

Figure 4.3 The relationship between the depth of the scour and the diameter of the single cylindrical pier when (Q=30 l/sec).

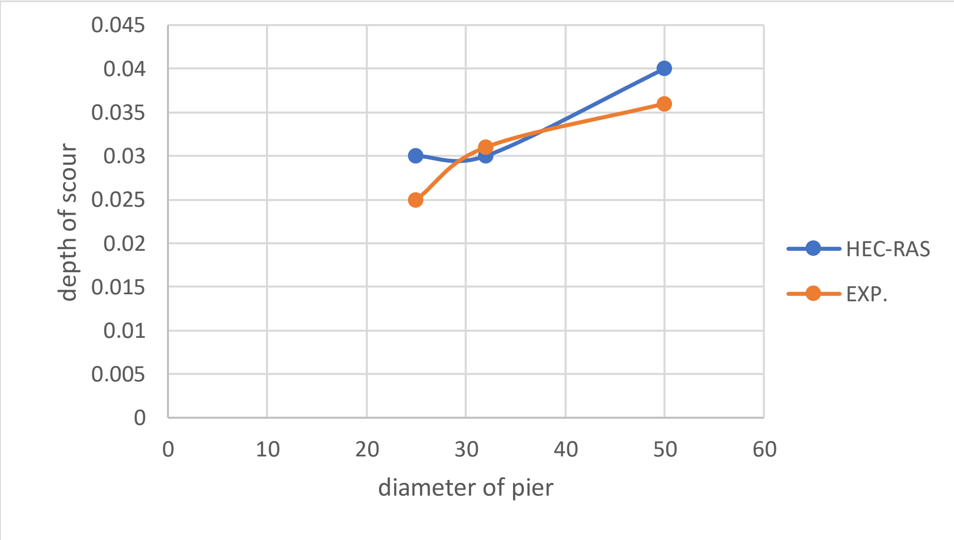

Figure 4.4 The relationship between the depth of the scour and the diameter of the single cylindrical pier when (Q=20 l/sec).

The lowest value of scour, which was (30) mm, was measured at a pier with a diameter of (25) mm and a discharge rate of (20 l/sec) as shown in Figure (4-5).

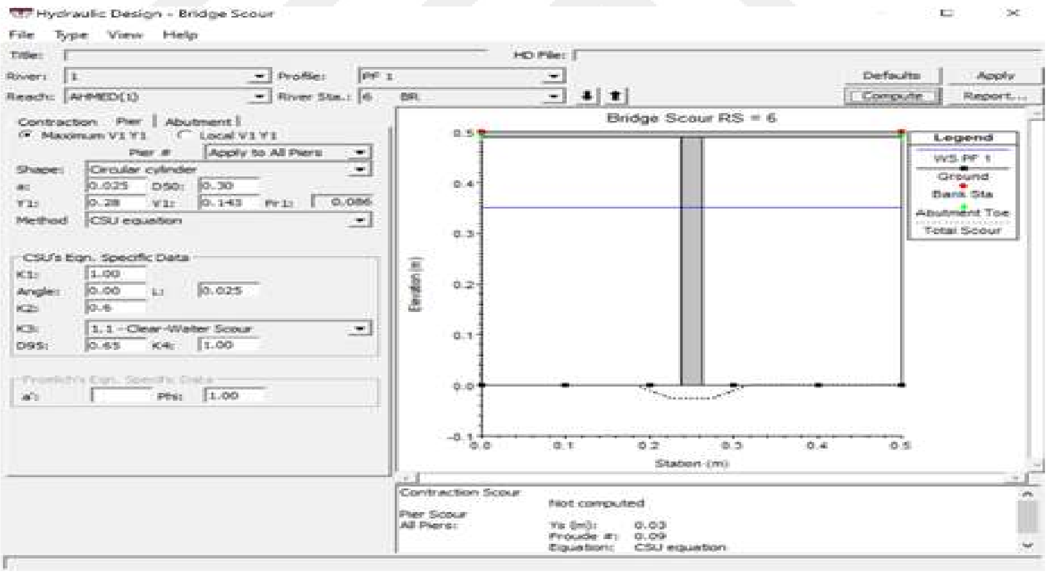

Figure 4.5 A typical run of numerical model (Run-No.1).

This is in line with what (Akhlaghi,2020) and (Alabi,2006) mentioned, the diameter of the Pier has an impact on the quantity of scouring that occurs as well as how long it takes for the scouring hole. In addition, it is noted that at the Pier with a diameter of (25) mm, the increase in discharge from (20 to 40) l/sec did not cause any increase in Scouring, and the depth of Scouring increased from (40 to 50)mm at the Pier with a diameter of (50) mm, the percentage increase was equal to (25%), indicating that doubling the diameter of the Pier and doubling the discharge increased the depth of Scouring. Figures (4-6), (4-7), and (4-8) depict the scouring that took place in the middle of the channel around single cylindrical piers with diameters of (32, and 50) mm, respectively.

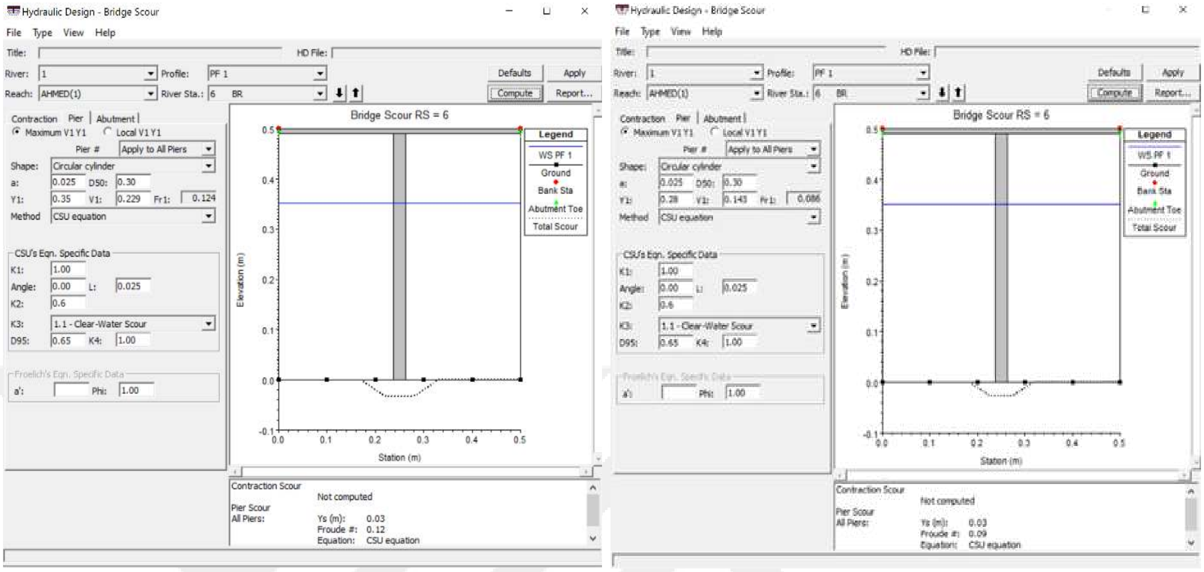

Figure 4.6 A typical run of numerical model (Run-No.1 and No.3).

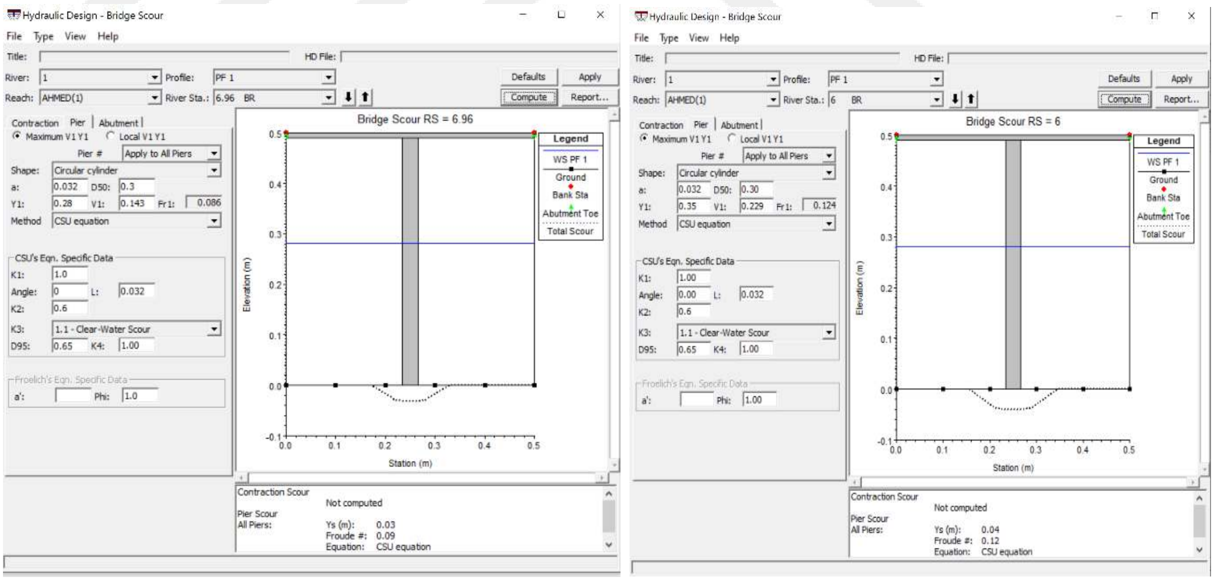

Figure 4.7 A typical run of the numerical model (Run-No.4 and No.6).

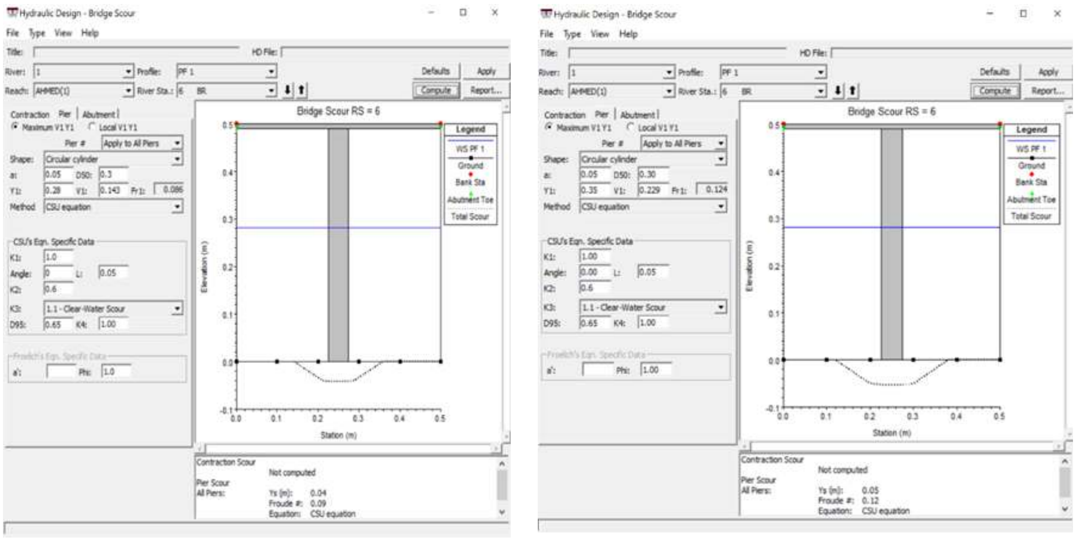

Figure 4.8 A typical run of the numerical model (Run-No.7 and No.9).

In the Group of cylindrical Piers 27 experiments were conducted, The diameter of the piers was varied three times (50, 32, and 25 mm) for each group of three consecutive cylindrical piers, and the distance between the piers was varied three times (2D,3D,4D) (D is the diameter of the pier). Three separate discharges of (20, 30, and 40) l/sec were passed for each of the previous cases as shown in, Figure (4-9).

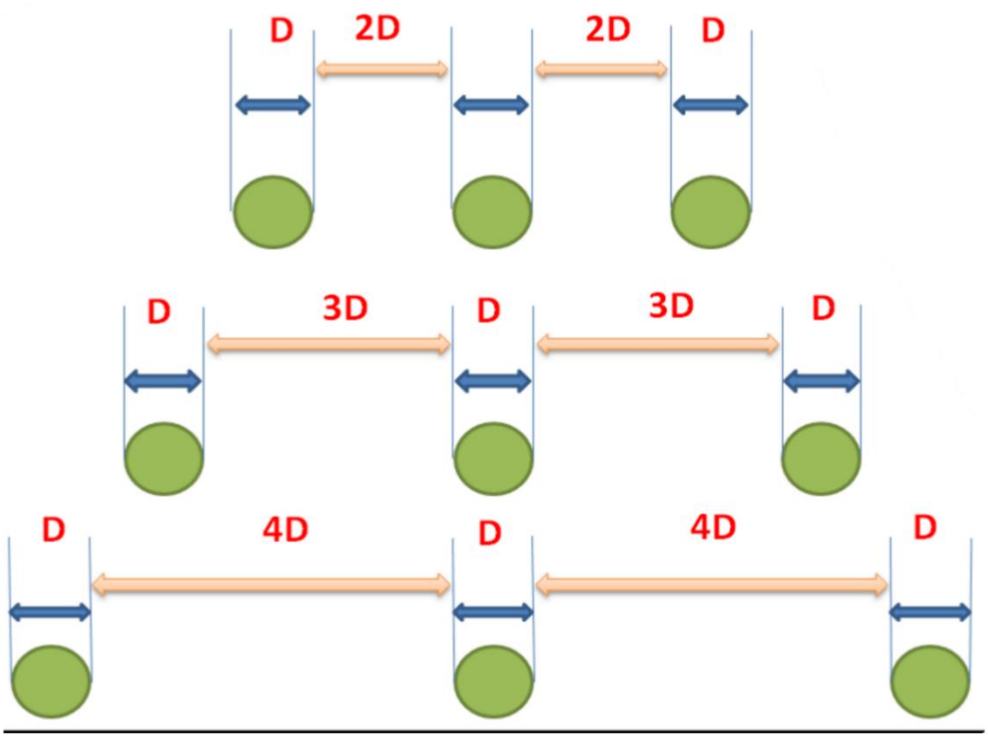

Figure 4.9 The dimensions of the successive piers and the distances used between them.

The table (4-2) displays the outcomes of various tests, both those of the program (HEC-RAS) and the actual experiments. The findings for these cases indicated that the front of the front piers experience varying amounts of maximum scouring when drainage is constant. The results of the simulation process also showed that for pavements with the same diameter, the drying at the front of the pavements increases with the increase of the discharge. However, it was observed through the results that the distance between the supports does not affect the depth of the scour when the discharge changes for the same diameter of the support However, it was observed through the laboratory results that the distance between the supports increases the depth of scouring when the discharge changes for the same diameter of the support.

Table 4.2 Results of scour around group cylindrical piers

Fr	D (mm)	S (mm)	Q (l/sec)	y (m)	V (m/sec)	S/y	D/y	Ds $_{Hec-Ras}$ (m)	D$_{s\ Hec-Ras}$/y	D$_{s\ exp.}$
0.086	25	50	0.02	0.28	0.143	0.179	0.089	0.03	0.107	0.025
0.111	25	50	0.03	0.31	0.194	0.161	0.081	0.03	0.097	0.030
0.123	25	50	0.04	0.35	0.229	0.143	0.071	0.03	0.086	0.034
0.086	25	75	0.02	0.28	0.143	0.268	0.089	0.03	0.107	0.023
0.111	25	75	0.03	0.31	0.194	0.242	0.081	0.03	0.097	0.028
0.123	25	75	0.04	0.35	0.229	0.214	0.071	0.03	0.086	0.031
0.086	25	100	0.02	0.28	0.143	0.357	0.089	0.03	0.107	0.022
0.111	25	100	0.03	0.31	0.194	0.323	0.081	0.03	0.097	0.025
0.123	25	100	0.04	0.35	0.229	0.286	0.071	0.03	0.086	0.029
0.086	32	64	0.02	0.28	0.143	0.229	0.114	0.03	0.107	0.030
0.111	32	64	0.03	0.31	0.194	0.206	0.103	0.04	0.129	0.038
0.123	32	64	0.04	0.35	0.229	0.183	0.091	0.04	0.114	0.046
0.086	32	96	0.02	0.28	0.143	0.343	0.114	0.03	0.107	0.029
0.111	32	96	0.03	0.31	0.194	0.310	0.103	0.04	0.129	0.033
0.123	32	96	0.04	0.35	0.229	0.274	0.091	0.04	0.114	0.041
0.086	32	128	0.02	0.28	0.143	0.457	0.114	0.03	0.107	0.027
0.111	32	128	0.03	0.31	0.194	0.413	0.103	0.04	0.129	0.030
0.123	32	128	0.04	0.35	0.229	0.366	0.091	0.04	0.114	0.037

Continue Table 4.2

0.086	50	100	0.02	0.28	0.143	0.357	0.179	0.04	0.143	0.035
0.111	50	100	0.03	0.31	0.194	0.323	0.161	0.05	0.161	0.052
0.123	50	100	0.04	0.35	0.229	0.286	0.143	0.05	0.143	0.063
0.086	50	150	0.02	0.28	0.143	0.536	0.179	0.04	0.143	0.035
0.111	50	150	0.03	0.31	0.194	0.484	0.161	0.05	0.161	0.042
0.123	50	150	0.04	0.35	0.229	0.429	0.143	0.05	0.143	0.060
0.086	50	200	0.02	0.28	0.143	0.714	0.179	0.04	0.143	0.033
0.111	50	200	0.03	0.31	0.194	0.645	0.161	0.05	0.161	0.039
0.123	50	200	0.04	0.35	0.229	0.571	0.143	0.05	0.143	0.057

Results from simulations for consecutive cylindrical piers are shown in Figure (4-10). For instance, the depth of scouring increases from (30 mm) when using the diameter of the piers (25) mm to (40 mm) when the diameter is (50) mm or a percentage increase of (25%) when the discharge is (20 l/sec) and the distance between the piers is equal to four times the diameter of the support (4D). The results showed that the increase is (25%) and (25%), respectively, when the distances between the supports are (3 d) and (2 d). As for the practical results when a discharge of (20) l/sec is passed, the increase in the diameter of the Piers from (25 to 50) mm leads to an increase in scouring by a percentage (44.2%,52.9%,49.7%) in a row when the distance between the supports changes from (2d,3d,4d).

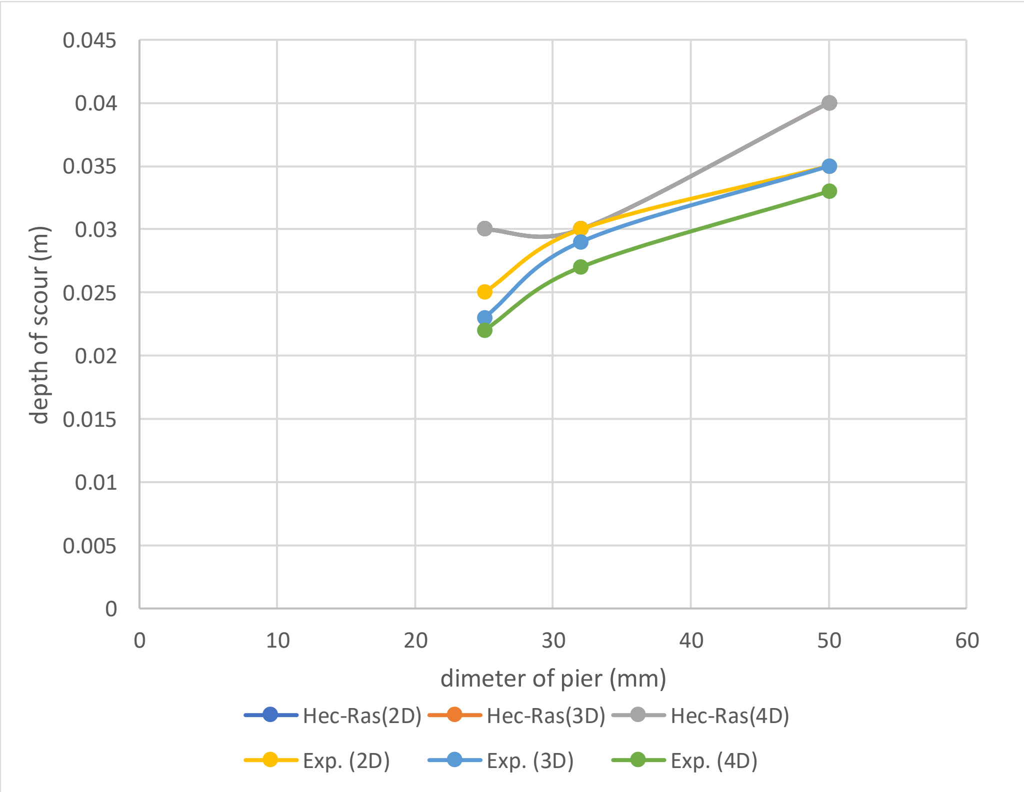

Figure 4.10 The relationship between the depth of scour and the diameter of the group cylindrical pier when (Q=20 l/sec).

As for the results from simulations for consecutive cylindrical piers are shown in Figure (4-11) the depth of scouring increases from (30 mm) when using the diameter of the piers (25) mm to (50 mm) when the diameter is (50) mm or a percentage increase of (40%) when the discharge is (30 l/sec) and the distance between the piers is equal to four times the diameter of the support (4D). According to the simulation's findings, the rate of increase for distances of (2D and 3D) is (25% and 40%), respectively. As for the practical results when a discharge of (30) l/sec is passed, the increase in the diameter of the Piers from (25 to 50) mm leads to an increase in scouring by a percentage (72%,46%,57%) in a row when the distance between the supports changes from (2d,3d,4d).

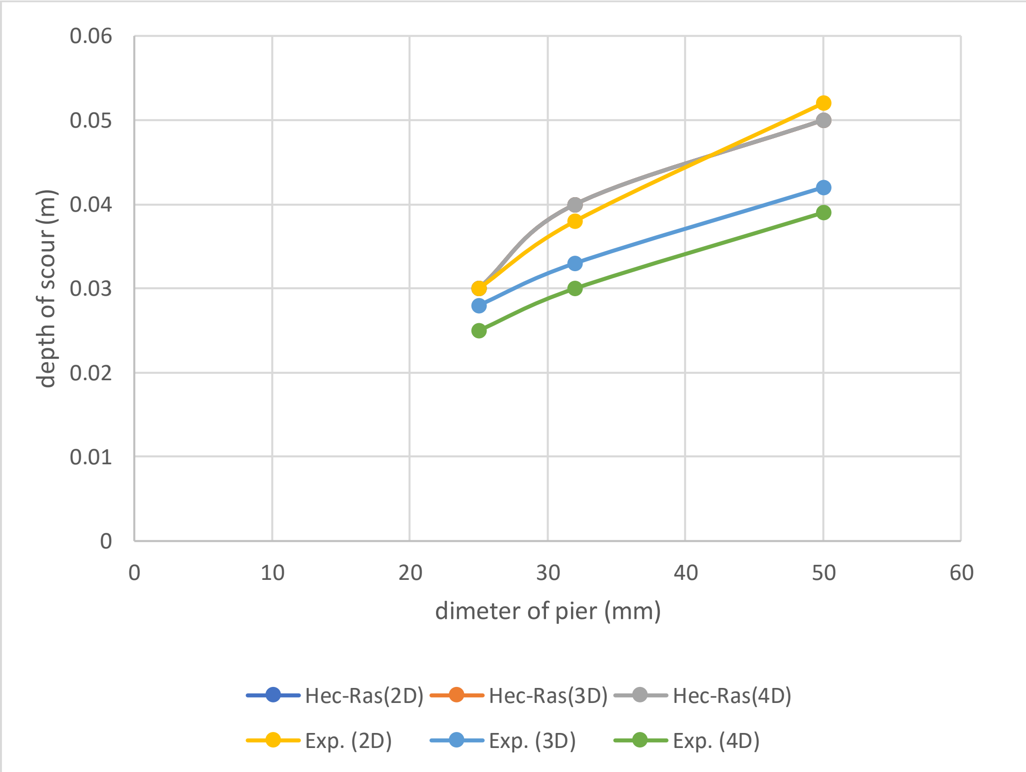

Figure 4.11 The relationship between the depth of the scour and the diameter of the group cylindrical pier when (Q=30 l/sec)

The same is the case when draining, the depth of scouring increases from (30)mm when using the diameter of the supports (25) mm to (50) mm when the diameter is (50) mm or a percentage increase of (40%) when the discharge is (40) liters per second and the distance between the supports is equal to four times the diameter of the support (4D). The results showed that the increase is (40%) and (25%), respectively, when the distances between the supports are (3 d) and (2 d).

As for the practical results when a discharge of (40) l/sec is passed, the increase in the diameter of the Piers from (25 to 50) mm leads to an increase in scouring by a percentage (83.7%,94.4%,93%) in a row when the distance between the supports changes from (2d,3d,4d).

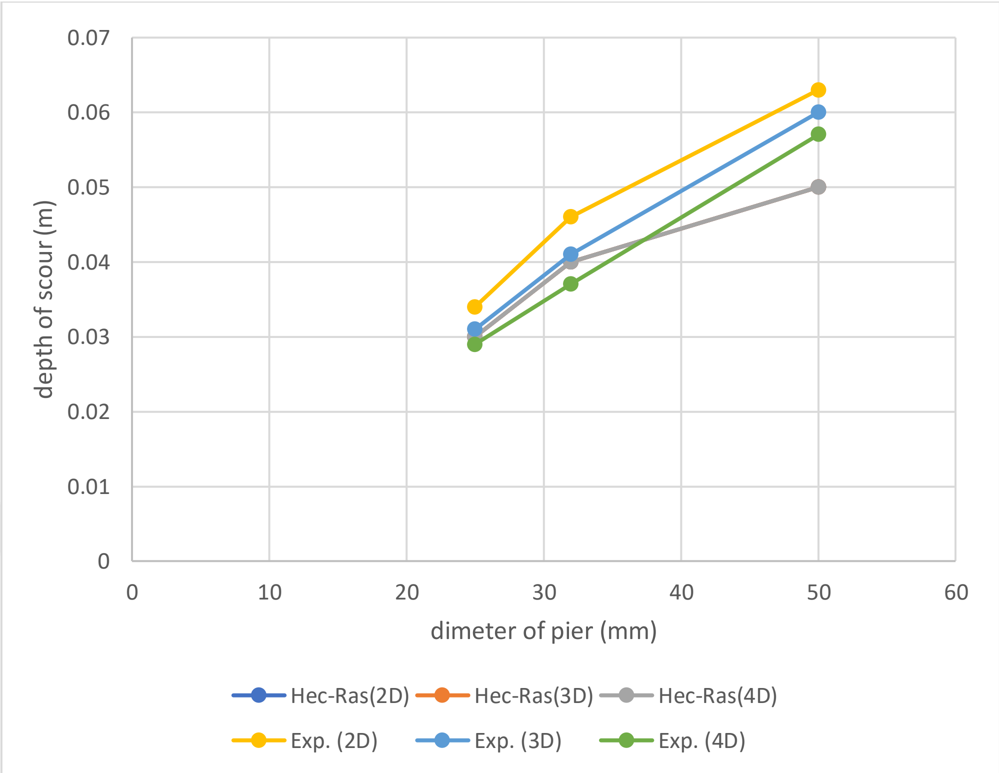

Figure 4.12 The relationship between the depth the of scour and the diameter of the group cylindrical pier when (Q=40 l/sec)

Figures (4-13) to (4-15) depict the scouring that takes place in the canal's middle section around a series of cylindrical piers, each with a diameter of (50)mm, when the distances between them are (2D) and for three different discharge rates of (20,30,40) l/sec, respectively. These figures show that the front of the cylindrical Piers, where scouring occurs to its greatest depth, varies in depth depending on the diameter of the Piers and the drainage that flows through the channel.

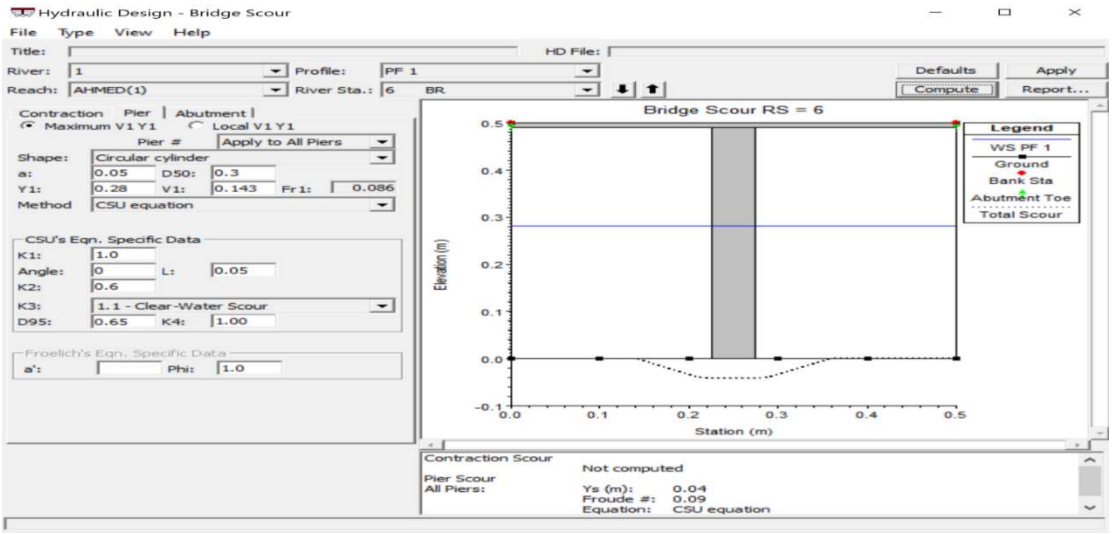

Figure 4.13 A typical run of numerical model (Run-No.10)

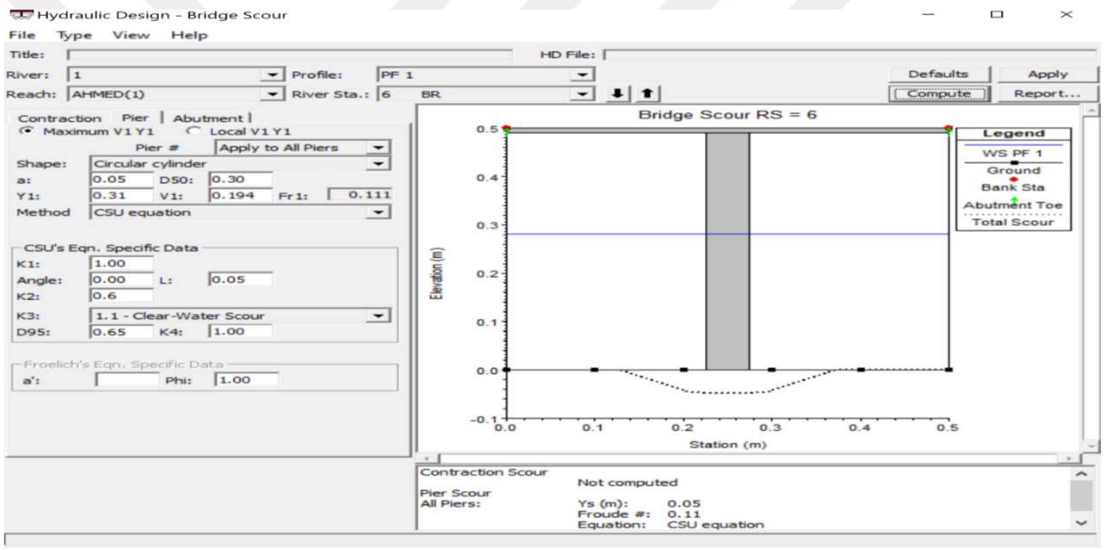

Figure 4.14 A typical run of numerical model (Run-No.11)

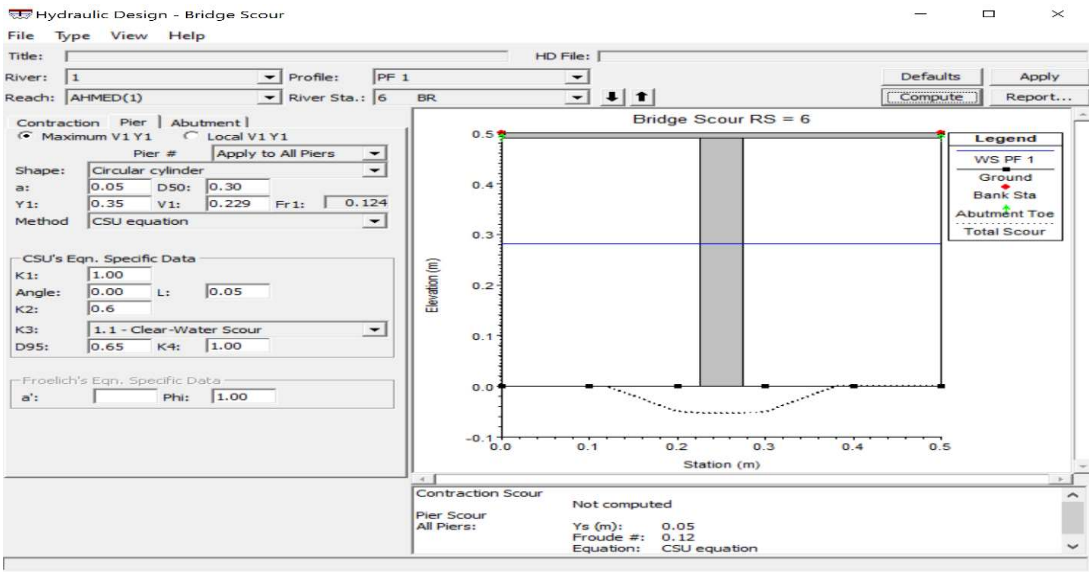

Figure 4.15 A typical run of numerical model (Run-No.12)

4.3.2 The Effect Depth of Flow on Depth Of Scour

The process of scouring the bottom soil around the piers grows with an increase in runoff because an increase in drainage causes an increase in flow depth. It has been noted (Richardson,2001) that the depth of runoff directly affects the depth of scouring since an increase in runoff can increase by scouring depth that is twice as deep or greater. The link between the depth of runoff and the depth of scouring for three different Pier diameters is depicted in Figure (4-16) for both simulation and practical experiments.

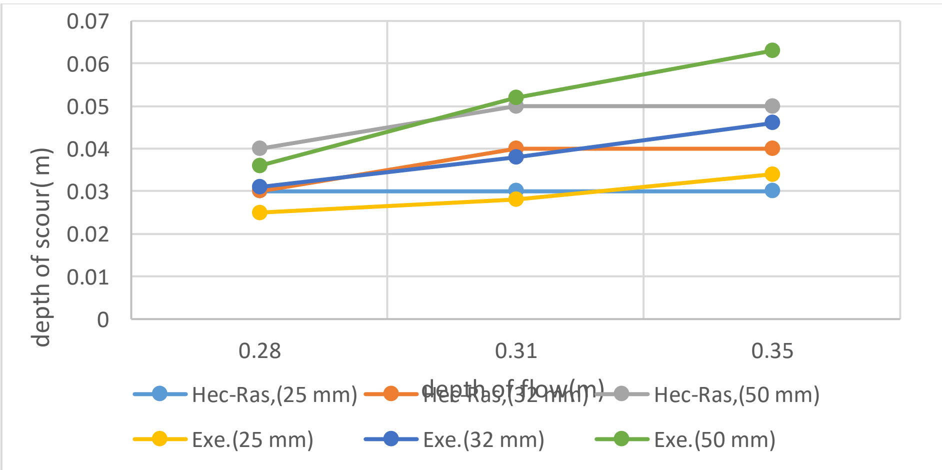

Figure 4.16 The relationship between the depth of scour and the Depth of flow on the single cylindrical pier.

It can be seen from this graph that the maximum amount of scouring, (50) mm, happened near a pier with a diameter of (50) mm and at a discharge of (40) liters/second, which caused a flow depth of (35) cm and when The discharge is (20) l/ sec, was shed for drainage at a depth of (28) cm, and this is when the bottom soil around this pier saw the lowest rate of scouring, which was equal to (30) mm. As for practical experiments, it was the highest value for scouring (63.12)mm. Similar results were found for the erosion around piers with diameters of (32) mm and (25) mm, where the largest and lowest scouring was measured at flow depths of (35) cm and (28) cm, respectively. For various situations of the diameter of the subsequent cylindrical piers as well as various examples of the distances between these piers, Figure (4-17) illustrates the link between the depth of scour and the depth of flow when the diameter of the pier (50) mm for group cylindrical pier.

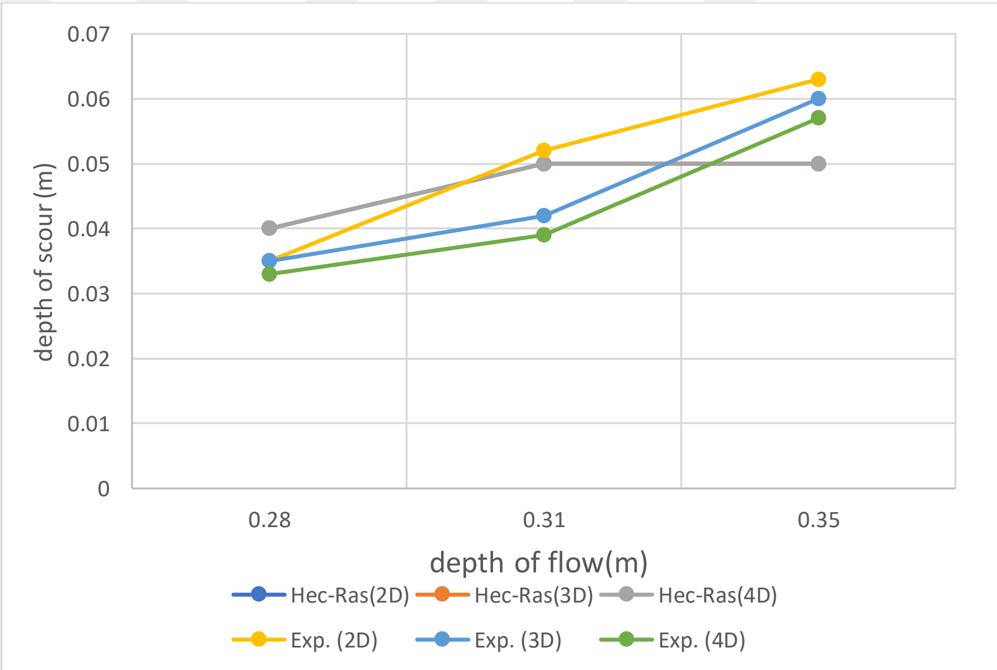

Figure 4.17 The relationship between the depth of scour and the Depth of flow on the group cylindrical pier when the diameter of the pier (50) mm.

4.3.3 The Effect Velocity of Flow on Depth of Scour

According to (Breusers, et al.,1977), scouring occurs in clear water circumstances when ($0.5 \leq \frac{Vc}{V} \leq 1$). Since ($\frac{Vc}{V}$) was more than (0.5) and less than (1). All actual and simulated tests for this study fall within these bounds. The relationship between the depth of scour and the flow velocity around single cylindrical piers with various diameters is depicted in Figure (4-18). The highest value of scour while utilizing a pier with a diameter of (50) mm is (50) mm at a flow velocity of (0.228) m/sec, and the lowest value of scour of soil is (30) mm at a velocity of (0.142) m/sec. However, when utilizing piers with diameters of (32) mm and (25) mm, respectively, the largest and lowest depth of scour at the two aforementioned flow retiaries (40 and 30) mm and (30) mm. This indicates that for the piers (50), (32) mm, and (25) mm, respectively, an increase in flow velocity of (60%) or (from 0.142 to 0.228) m/sec results in an increase in the depth of scour of (20%), (25%), and (25%), respectively. As for the practical experiments, the increase in flow velocity of (60%) or (from 0.142 to 0.228) m/sec results in an increase in the depth of scour of (72%), (48.26%) and (35.11%) for piers with a diameter of (50,32,25) mm, respectively.

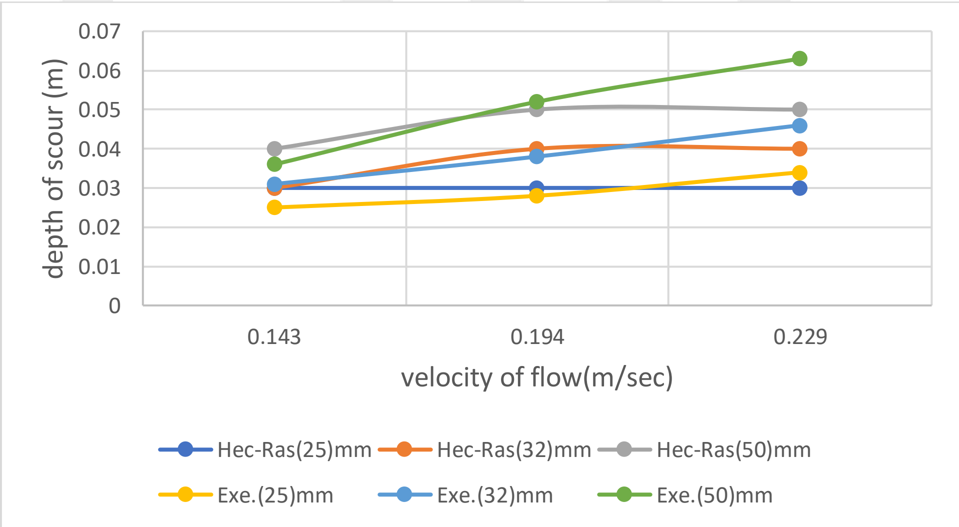

Figure 4.18 The Relationship Between The Depth Of Scour and The Velocity Of Flow On The Single Cylindrical Pier.

This means that increasing the flow velocity by (60%) causes the depth of scouring to increase by a factor of two when the diameter of the cylindrical pier doubles (from 25 to 50 mm). The relationship between the flow velocity and the depth of scour around the consecutive cylindrical piers is shown in figure (4-19). This figure shows that the depth of scour also rises as flow velocity rises and that employing larger diameter piers results in the greatest depth of scour. For instance, it is stated that the increase in speed from (0.142) to (0.228) m/sec is the proportion of the rise in scour (20%) while employing piers with a diameter of (50) mm and the distance between the piers is (2D). While utilizing piers with a diameter of (32) mm and (25) mm, respectively, and the distance between these piers is also (2D), the percentage of increase in scour is (25%) and (25%), respectively. As for the practical experiments, the increase in flow velocity of (60%) or (from 0.142 to 0.228) m/sec and the distances between pier (2D) results in an increase in the depth of scour of (75.81%), (52.78%) and (36.66%) for piers with a diameter of (50,32 and 25) mm, respectively.

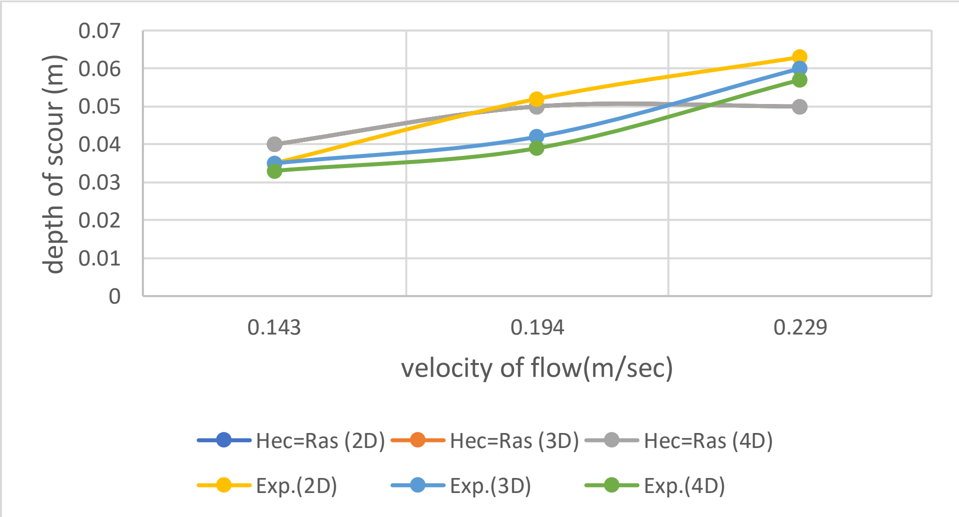

Figure 4.19 The relationship between the depth of scour and the flow velocity on the group cylindrical pier when the diameter of the pier (50) mm.

It is important to note that the findings supported the researchers' claims (Chabert and Engeldiger, 1956), (Breusers, et al.,1977), (Ettema, 1980) and (Chiew,1984) that the relationship between the depth of scour and the velocity of runoff or the depth of runoff is linear for all piers, whether single or in succession.

4.4 Scouring Around Rectangular Piers With Semi-circular Ends

One of the key elements that significantly contributes to the development and power of the vortex system is the design of the pier. In this study, rectangular piers with semi-circular ends were simulated in addition to the circular piers to demonstrate how the depth and shape of the pit of scour change. Pier bridges are built in a variety of configurations. When employing these piers, replace the succeeding cylindrical piers so that their combined length equals the distance between the first pier's front face and the last pier's back face. The dimensions of the piers employed in this study are schematically shown in Figure (4-20), with the choice of cylindrical piers with a diameter of (50) mm made because they caused the greatest depth of scour to occur when passing through the various drains (Kirkil, Constantinescu, & Ettema, 2005).

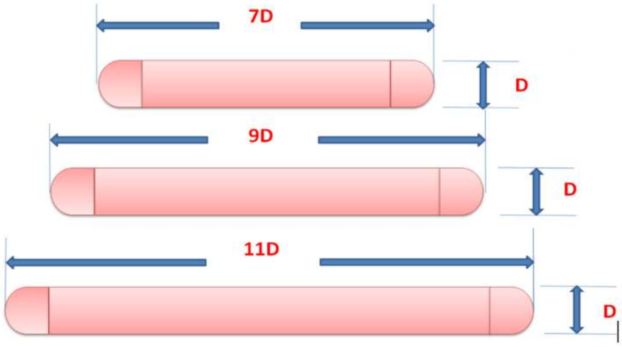

Figure 4.20 Dimensions of rectangular piers with semicircular ends.

The rectangular pier with a semi-circular end will have a length of (7D) when the space between the succeeding piers is equal to (2D). Thus, the length of the rectangular pier with the semi-circular end will be (9D) and (11D), respectively, when the distance between the piers is (3D) and (4D). For practical studies, scour around these piers occurred when drainage flowed by them at a rate of (40) l/ sec, with a maximum depth of (60.31,56.27, and 52.11) mm, respectively. Figure (4-21) shows the scour hole for the pier. However, the outcomes of the simulation when run with the (HEC-RAS) program are (50) mm for all lengths. That is when comparing the pier with length (11D) with subsequent piers with a diameter of (50) mm and the distance between the piers (4D), these piers caused an increase in the depth of scour by (5.03%). While a comparison of the pier with length (9D) With subsequent piers with a diameter of (50) mm and a distance of (3D) revealed a decrease in the depth of scour by (7.02%), When comparing the pier with a length of (7 d) with subsequent piers with a diameter of (50) mm and the distance between them (2D), the depth of scour also decreased by (17.39%). According to the simulation's findings, the successive cylindrical piers and the rectangular piers with circular ends always have similar depths of scouring (Klingeman, 1973).

Figure 4.21 Scour holes for the pier with semicircular ends.

4.5 Scouring Around Cylindrical Piers for Three Forms

Three different pier shapes were the subject of 81 trials. 27 experiments were carried out for each of these forms (A, B, and C) to determine how the scouring around these piers changed. As depicted in Figure (4-22), three different water discharges (20,30 and 40) L/sec were made. The highest value of scouring happened in Figure (A) and its value was (60) mm at the discharge (40) L/sec and the diameter of the pillar (50) mm. The highest value of scouring of the piers was taken in each trial, and the findings were close to some extent.

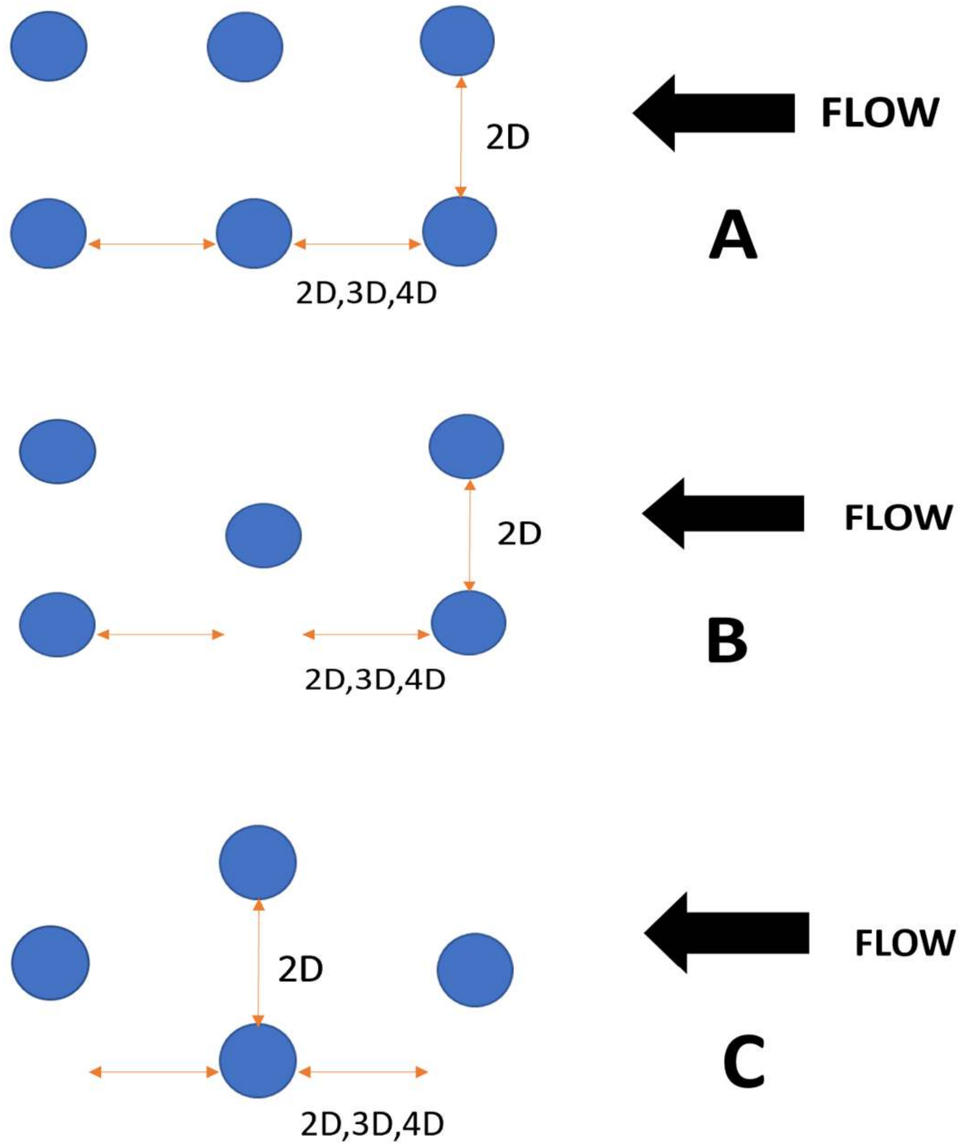

Figure 4.22 Three Different Forms (A, B, and C).

The maximum value of scouring around the piers for the three figures occurred at the piers with the highest water discharge (40 l/sec), the largest diameter (50 mm), and the closest spacing between them. According to tables (4-3), (4-4), and (4-5) for the three figures, respectively.

Table 4.3 Results of scour around group cylindrical piers for shape (A)

D (mm)	Q (l/sec)	SH (mm)	Fr	y (m)	SH/Y	V (m/sec)	$ds_{(hec)}/y$	$ds_{(hec)}$ (m)
25	20	50	0.086	0.28	0.179	0.143	0.107	0.03
		75	0.086	0.28	0.268	0.143	0.107	0.03
		100	0.086	0.28	0.357	0.143	0.107	0.03
	30	50	0.111	0.31	0.161	0.194	0.097	0.03
		75	0.111	0.31	0.242	0.194	0.097	0.03
		100	0.111	0.31	0.323	0.194	0.097	0.03
	40	50	0.123	0.35	0.143	0.229	0.114	0.04
		75	0.123	0.35	0.214	0.229	0.086	0.03
		100	0.123	0.35	0.286	0.229	0.086	0.03
32	20	64	0.086	0.28	0.229	0.143	0.107	0.03
		96	0.086	0.28	0.343	0.143	0.107	0.03
		128	0.086	0.28	0.457	0.143	0.107	0.03
	30	64	0.111	0.31	0.206	0.194	0.129	0.04
		96	0.111	0.31	0.310	0.194	0.129	0.04
		128	0.111	0.31	0.413	0.194	0.097	0.03
	40	64	0.123	0.35	0.183	0.229	0.143	0.05
		96	0.123	0.35	0.274	0.229	0.114	0.04
		128	0.123	0.35	0.366	0.229	0.114	0.04
50	20	100	0.086	0.28	0.357	0.143	0.143	0.04
		150	0.086	0.28	0.536	0.143	0.143	0.04
		200	0.086	0.28	0.714	0.143	0.107	0.03
	30	100	0.111	0.31	0.323	0.194	0.161	0.05
		150	0.111	0.31	0.484	0.194	0.129	0.04
		200	0.111	0.31	0.645	0.194	0.129	0.04
	40	100	0.123	0.35	0.286	0.229	0.171	0.06
		150	0.123	0.35	0.429	0.229	0.171	0.06
		200	0.123	0.35	0.571	0.229	0.171	0.06

Table 4.4 Results of scour around group cylindrical piers for shape (B)

D (mm)	Q (l/sec)	SH (mm)	Fr	y (m)	SH/Y	V (m/sec)	$ds_{(hec)}/y$	$ds_{(hec)}$ (m)
25	20	50	0.086	0.28	0.179	0.143	0.107	0.03
		75	0.086	0.28	0.268	0.143	0.107	0.03
		100	0.086	0.28	0.357	0.143	0.107	0.03
	30	50	0.111	0.31	0.161	0.194	0.097	0.03
		75	0.111	0.31	0.242	0.194	0.097	0.03
		100	0.111	0.31	0.323	0.194	0.097	0.03
	40	50	0.123	0.35	0.143	0.229	0.086	0.03
		75	0.123	0.35	0.214	0.229	0.086	0.03
		100	0.123	0.35	0.286	0.229	0.086	0.03
32	20	64	0.086	0.28	0.229	0.143	0.107	0.03
		96	0.086	0.28	0.343	0.143	0.107	0.03
		128	0.086	0.28	0.457	0.143	0.107	0.03
	30	64	0.111	0.31	0.206	0.194	0.129	0.04
		96	0.111	0.31	0.310	0.194	0.129	0.04
		128	0.111	0.31	0.413	0.194	0.097	0.03
	40	64	0.123	0.35	0.183	0.229	0.114	0.04
		96	0.123	0.35	0.274	0.229	0.114	0.04
		128	0.123	0.35	0.366	0.229	0.114	0.04
50	20	100	0.086	0.28	0.357	0.143	0.143	0.04
		150	0.086	0.28	0.536	0.143	0.143	0.04
		200	0.086	0.28	0.714	0.143	0.107	0.03
	30	100	0.111	0.31	0.323	0.194	0.161	0.05
		150	0.111	0.31	0.484	0.194	0.129	0.04
		200	0.111	0.31	0.645	0.194	0.129	0.04
	40	100	0.123	0.35	0.286	0.229	0.171	0.06
		150	0.123	0.35	0.429	0.229	0.171	0.06
		200	0.123	0.35	0.571	0.229	0.143	0.05

Table 4.5 Results of scour around group cylindrical piers for shape (C)

D (mm)	Q (l/sec)	SH (mm)	Fr	y (m)	SH/Y	V (m/sec)	$ds_{(hec)}/y$	$ds_{(hec)}$ (m)
25	20	50	0.086	0.28	0.179	0.143	0.107	0.03
		75	0.086	0.28	0.268	0.143	0.107	0.03
		100	0.086	0.28	0.357	0.143	0.107	0.03
	30	50	0.111	0.31	0.161	0.194	0.097	0.03
		75	0.111	0.31	0.242	0.194	0.097	0.03
		100	0.111	0.31	0.323	0.194	0.097	0.03
	40	50	0.123	0.35	0.143	0.229	0.086	0.03
		75	0.123	0.35	0.214	0.229	0.086	0.03
		100	0.123	0.35	0.286	0.229	0.086	0.03
32	20	64	0.086	0.28	0.229	0.143	0.107	0.03
		96	0.086	0.28	0.343	0.143	0.107	0.03
		128	0.086	0.28	0.457	0.143	0.107	0.03
	30	64	0.111	0.31	0.206	0.194	0.129	0.04
		96	0.111	0.31	0.310	0.194	0.129	0.04
		128	0.111	0.31	0.413	0.194	0.129	0.04
	40	64	0.123	0.35	0.183	0.229	0.114	0.04
		96	0.123	0.35	0.274	0.229	0.114	0.04
		128	0.123	0.35	0.366	0.229	0.114	0.04
50	20	100	0.086	0.28	0.357	0.143	0.143	0.04
		150	0.086	0.28	0.536	0.143	0.143	0.04
		200	0.086	0.28	0.714	0.143	0.143	0.04
	30	100	0.111	0.31	0.323	0.194	0.129	0.04
		150	0.111	0.31	0.484	0.194	0.129	0.04
		200	0.111	0.31	0.645	0.194	0.129	0.04
	40	100	0.123	0.35	0.286	0.229	0.143	0.05
		150	0.123	0.35	0.429	0.229	0.143	0.05
		200	0.123	0.35	0.571	0.229	0.143	0.05

4.6 Statistical Analysis Results

In this section, the non-dimensional factors result in the table (4-3), (4-4) and (4-5) were used to derive a position equation to calculate the maximum depth scouring around piers cylinders using the statistical program SPSS. This was done in light of what was discovered in equation (3-7) through dimensional analysis. According to the statistical analysis's findings, the following equations (3-8), (3-9), and (3-10) might be used to determine the depth of scour for each of the three types (A, B, C) in clear water with subcritical surface runoff respectively.

$$d_s = \frac{2.16 * D^{0.85} * y^{0.381} * F_r^{0.537}}{S^{0.231}} \quad \ldots\ldots\ldots\ldots\ldots\ldots\ldots\ldots(3\text{-}8)$$

The coefficient of determination (R^2) of this equation (3-8) is 0.905.

Where:

ds= maximum scour depth in (m)

y= depth of flow in (m)

Fr= Froude number (subcritical condition)

D = Roller pier diameter(m).

S = Distance between piers Consecutive (m).

$$d_s = \frac{1.857 * D^{0.916} * y^{0.279} * F_r^{0.401}}{S^{0.195}} \quad \ldots\ldots\ldots\ldots\ldots\ldots\ldots\ldots(3\text{-}9)$$

and for the coefficient of determination (R^2) of this equation (3-9) is 0.797.

$$d_s = \frac{1.463 * D^{0.842} * y^{0.318} * F_r^{0.377}}{S^{0.16}} \quad \ldots\ldots\ldots\ldots\ldots\ldots\ldots\ldots(3\text{-}10)$$

and for the coefficient of determination (R^2) of this equation (3-10) is 0.764.

Figures (4-23) to (4-25) show the relationship between (ds/D) calculated by HEC-RAS and measured by the above equations expected for scenarios (A, B, and C) respectively.

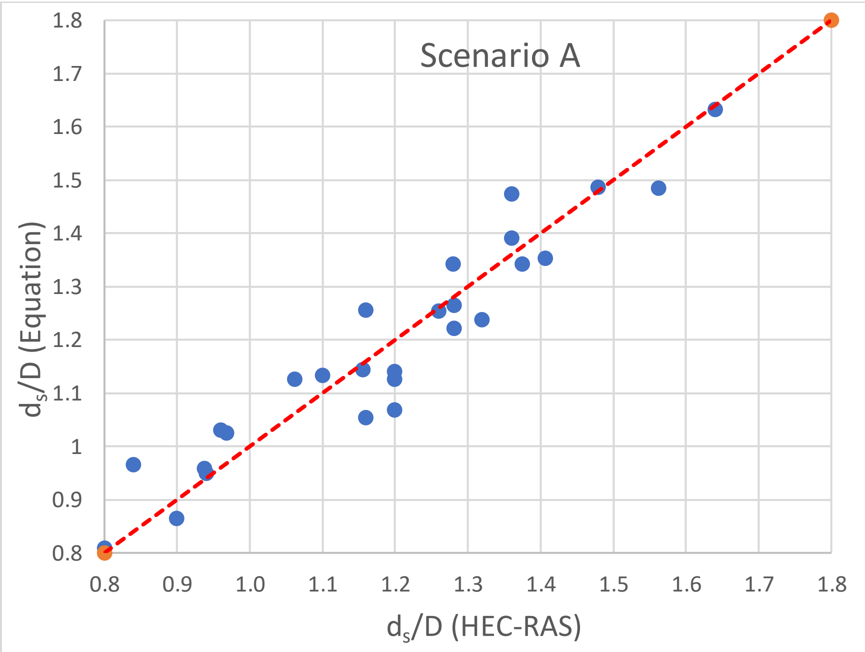

Figures 4.23 Relationship between calculated (ds/D) by HEC-RAS and measured by the predicted equation for scenario A.

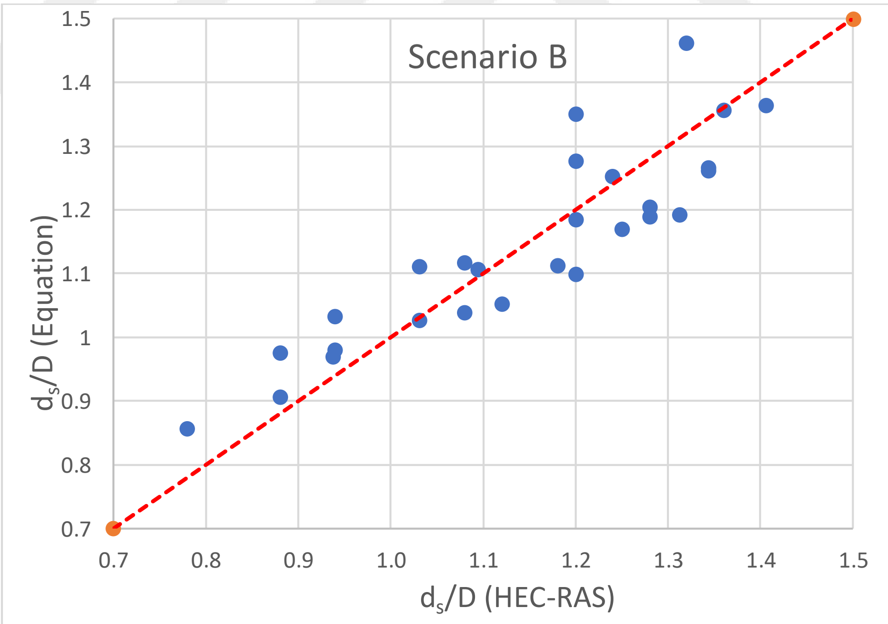

Figures 4.24 Relationship between calculated (ds/D) by HEC-RAS and measured by the predicted equation for scenario B.

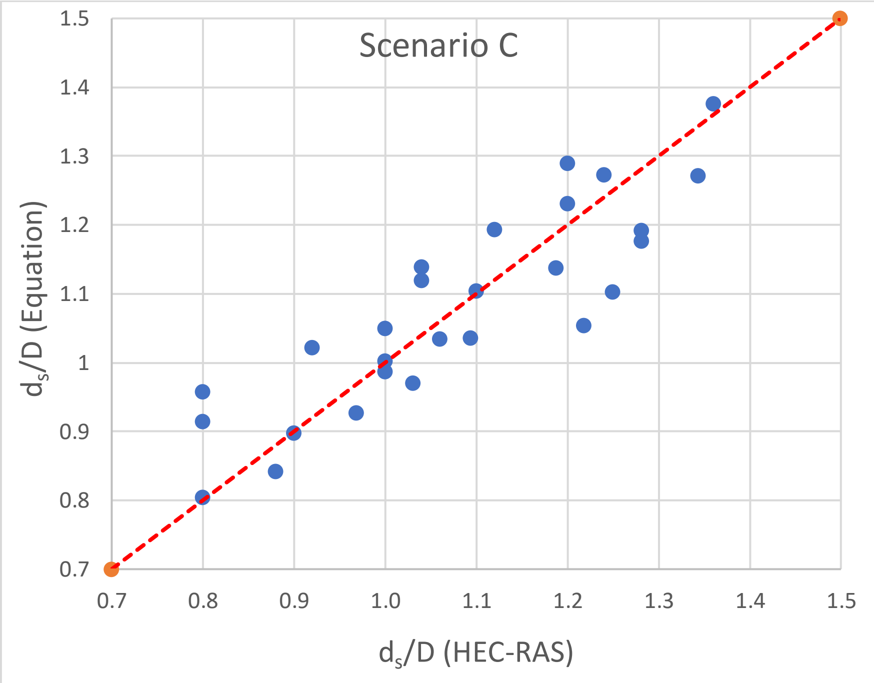

Figures 4.25 Relationship between calculated (ds/D) by HEC-RAS and measured by the predicted equation for scenario C.

Figures (4-26) to (4-34) show the relationship between the dimensionless cleanness parameter (ds/D) and cleanness distance parameter (S/D) for scenarios (A and B) for each of the three diameters.

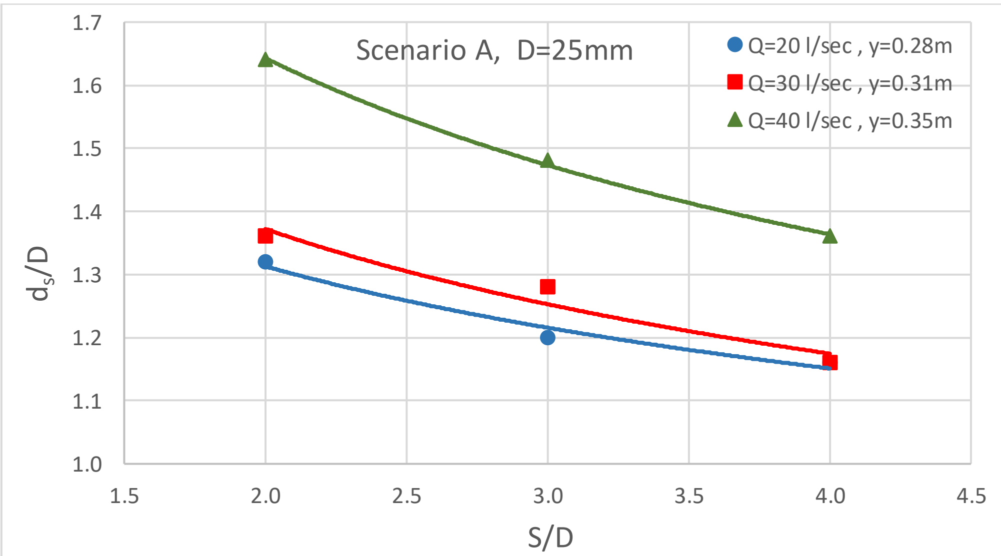

Figures 4.26 Relationship between dimensionless scour parameter (d_s/D) and dimensionless distance parameter (S/D) for scenario A and (D=25mm).

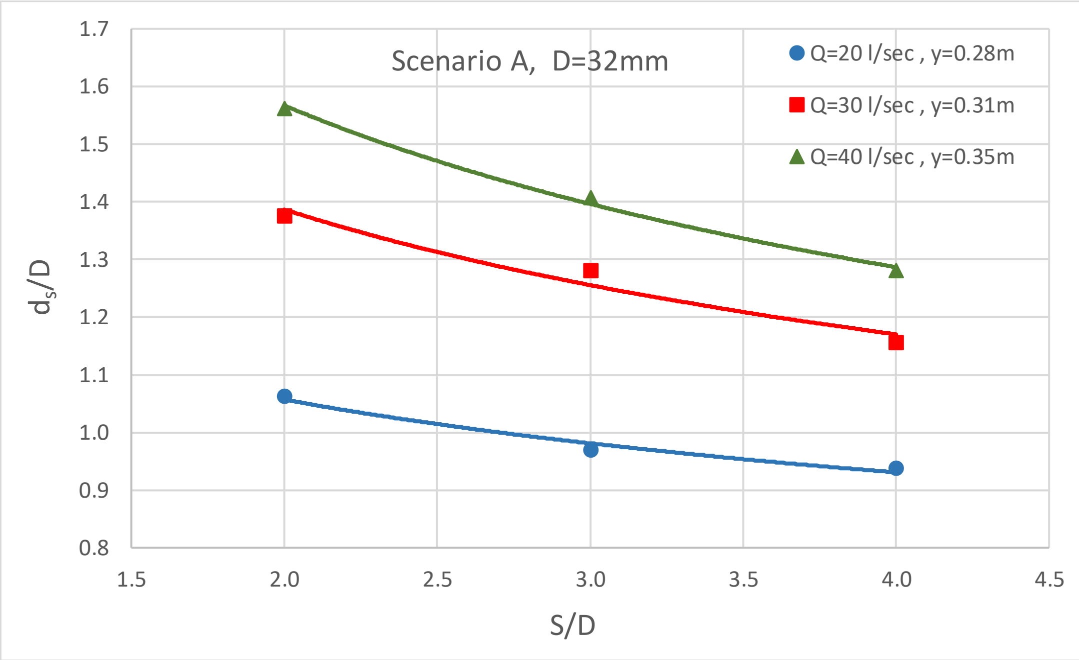

Figures 4.27 Relationship between dimensionless scour parameter (ds/D) and dimensionless distance parameter (S/D) for scenario A and (D=32mm).

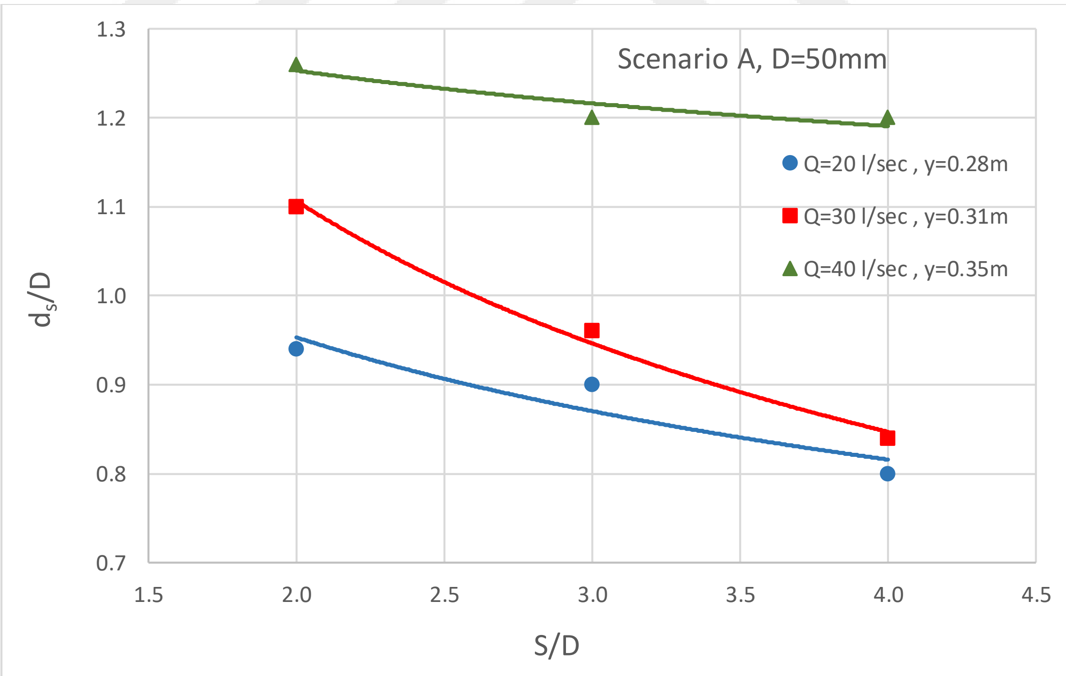

Figures 4.28 relationship between dimensionless scour parameter (ds/D) and dimensionless distance parameter (S/D) for scenario A and (D=50mm).

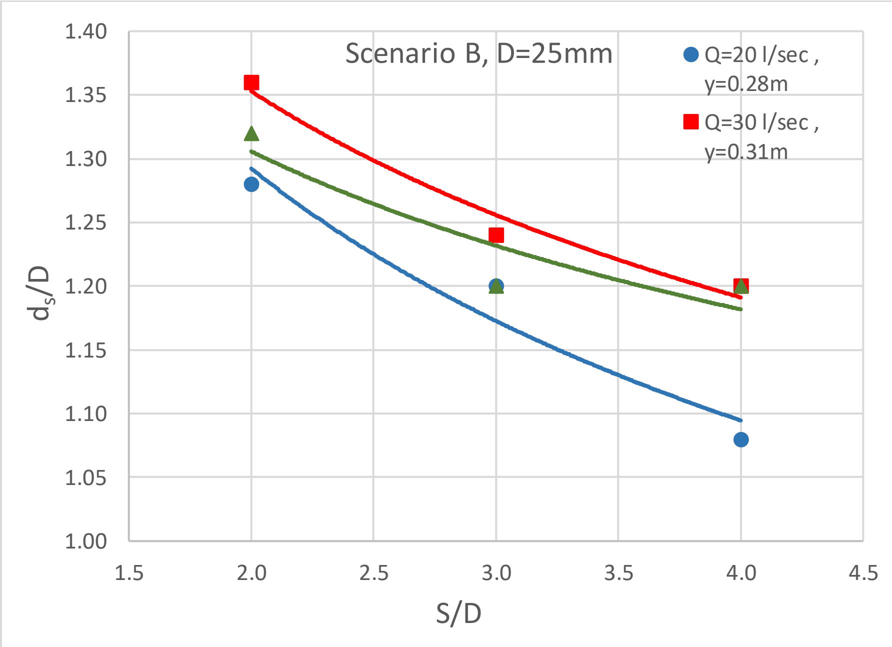

Figures 4.29 Relationship between dimensionless scour parameter (ds/D) and dimensionless distance parameter (S/D) for scenario B and (D=25mm).

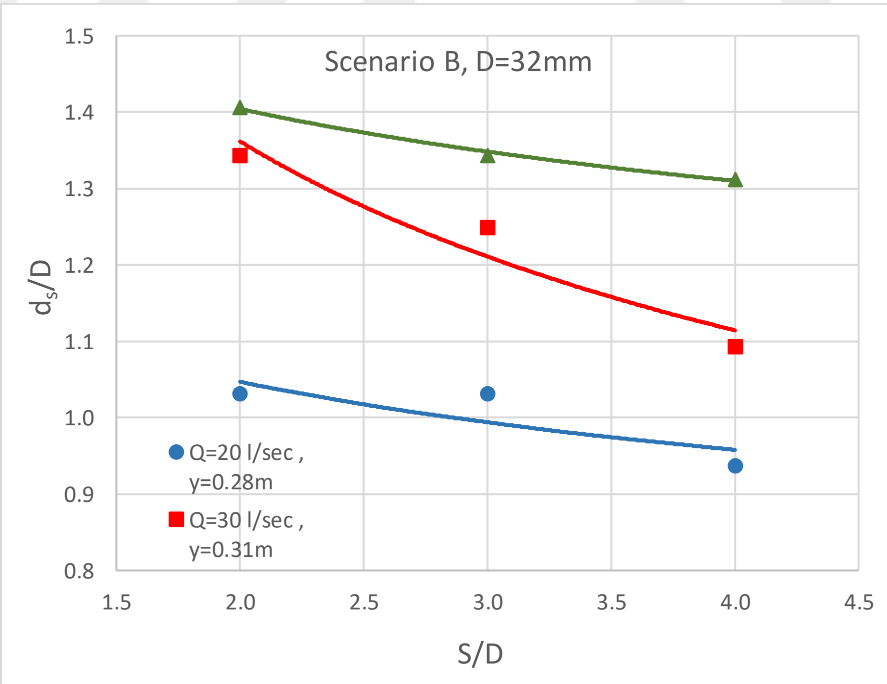

Figures 4.30. Relationship between dimensionless scour parameter (ds/D) and dimensionless distance parameter (S/D) for scenario B and (D=32mm).

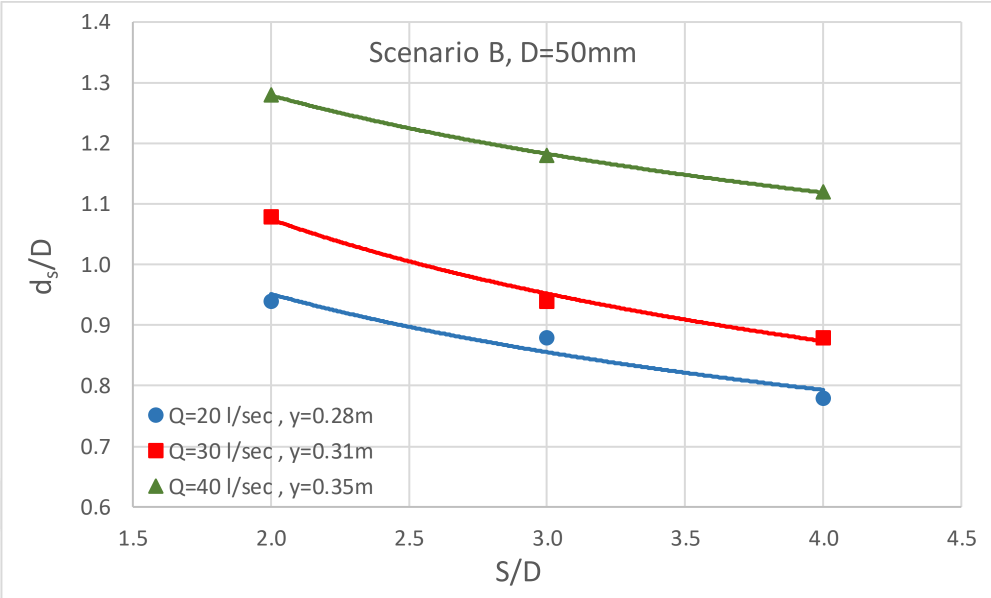

Figures 4.31. Relationship between dimensionless scour parameter (ds/D) and dimensionless distance parameter (S/D) for scenario B and (D=50mm).

CHAPTER 5

CONCLUSIONS AND RECOMMENDATIONS

5.1 Conclusions

In this study, three different types of piers (single cylindrical piers, successive cylindrical piers, and rectangular piers with circular ends) were compared in order to compare the results of scouring using the program (HEC-RAS) with those of in situ scouring of practical experiments. To achieve this, (45) simulated operations were carried out on these various pier shapes using the (HEC-RAS) program by varying the diameter of the piers, whether they were single or in succession, with varying the distance between the successive piers, as well as varying the width and length of the rectangular piers. knowing that the drainage was altered multiple times for each of these forms, and the flow complied with the requirements for pure water.

The following conclusions can be drawn from simulated findings of actual experiments:

1. When the flow variables (drainage and depth of flow) are proven, increasing the diameter of cylindrical piers—whether single or in succession—as well as rectangular piers with semi-circular ends causes an increase in scour around these piers. This is because the increased area of the runoff hitting the pier leads to an increase in the downward and growing flow, with Horseshoe swirls causing significant scouring.
2. The findings also indicated that increasing the diameter of the pier and the drainage surrounding single cylindrical piers both enhance the depth of scouring.
3. When the diameter of the pier remains constant, the depth of runoff has a direct impact on the depth of scour around the piers, increasing together with the runoff's depth. In situations where the piers have a modest diameter, the rise is progressive rather than hurried.
4. When doubling the diameter of the cylindrical pier (25 to 50 mm), the increase in the flow velocity (0.143 to 0.229 m/sec) leads to a doubling of the percentage increase in the depth

5. of scouring (50% to 75%) using simulation. As for the laboratory results using the same variables, the percentage of increase in the depth of scouring was (35% to 72%).
6. The results showed that for single and successive cylindrical piers, the relationship between the depth of erosion and flow velocity or the depth of the runoff is linear, and the slope of this relationship increases with the increase in the diameter of the support.
7. About rectangular abutments with semicircular ends, the depth of incision increases with the increase in the abutment diameter at the stability of the drain and the length of the abutment.
8. A simple and accurate positional equation was devised to calculate the maximum depth of etching around the cylindrical supports.
9. Through the use of the simulation program, the results of the cleaning depth were convergent with experimental results, and the shape of the affected section of the cleaning area was almost similar to the real shape of the cleaning area using the same variables. This difference is likely to be because the output of the (Hec-Ras) program is in unit (0.00 m).
10. Using the statistical program (SPSS) for the data of the (Hec-Ras) program, where circumstantial equations were deduced to calculate the depth of the scour, where the coefficient(R2) of determination of these equations, respectively, for shapes (A, B, and C) is (0.905, 0.797, 0.764).

5.2 Recommendations

1. It is necessary to test the effect of rectangular piers with rounded noses on the scour depth in cases of supercritical flow and then propose an empirical equation to calculate the scour depth within these conditions.
2. Studying the seam around piers of other shapes, whether single or group, with distances commensurate with forms of these supports.
3. A study of the use of successive cylindrical supports with different diameters and distances similar to this study when it is inclined at different angles with the direction of flow and compare its results with the results of this study.
4. The use of openings in the piers of different shapes and their effect on the depth of scour around piers.

5. Research the dispersion of vortices that cause scour in the front of the piers by suggesting specific arrangements in the pier at these areas, such as making protrusions of different lengths and showing their effect on the amount of depth Scour.

REFERENCES

Abdallah Mohamed, Y., & Abdel-Aal, M. G., Hemdan Nasr-Allah, T., & shawky, A.(2016). Experimental and theoretical investigation of scour at bridge abutmentAbdallah. *Journal of king saud university Engineering sciences, 28*, 32-40.

Akhlaghi, E., Babarsad, M. S., Derikvand, E., & Abedini, M. (2020). Assessment the effects of different parameters to rate scour around single piers and pile groups: a review. *Archives of Computational Methods in Engineering*, *27*(1), 183-197.

Akib, S., Liana Mamat, N., Basser, H., & Jahangirzadeh, A. (2014). Reducing local scouring at bridge piles using collars and geobags. *The Scientific World Journal, 2014*.

Akilli, H., Sahin, B., & Tumen, N. F. (2005). Suppression of vortex shedding of circular cylinder in shallow water by a splitter plate. *Flow Measurement and Instrumentation, 16*(4), 211-219.

Ali, T. M., & Ghazali, A. H. (2013). 2 Discussion of "Clear-Water Local Scour 3 around Pile Groups in Shallow-Water Flow" 4 by Ata Amini, Bruce W. Melville. *JOURNAL OF HYDRAULIC ENGINEERING, 1*.

Azizian, A., AmirTakoldani, A., & GholiZadeh, M. (2010). *bridge pier scour using Hex-Ras 4.0 numerical model.* Paper presented at the fifth national congress of civil engineering.

Burrell, B. C., Comfort, G., & Beltaos, S. (2023). Considerations in the Planning and Design of Bridges in Ice-Affected Rivers: A Review. *Canadian Journal of Civil Engineering*, (ja).

Breusers, H. N. C., Nicollet, G., & Shen, H. W. (1977). Local scour around cylindrical piers. *Journal of hydraulic research*, *15*(3), 211-252.

Dey, S., Sumer, B. M., & Fredsøe, J. (2006). Control of scour at vertical circular piles under waves and current. *JOURNAL OF HYDRAULIC ENGINEERING, 132*(3), 270-279.

Elnikhely, E. (2017). Minimizing scour around bridge pile using holes. *Ain Shams Engineering Journal, 8*(4), 499-506.

Ettema, R. (1980). Scour at bridge piers.

Ettema, R., Melville, B. W., & Barkdoll, B. (1998). Scale effect in pier-scour experiments. *JOURNAL OF HYDRAULIC ENGINEERING, 124*(6), 639-642.

Grimaldi, C., Gaudio, R., Calomino, F., & Cardoso, A. H. (2009). Control of scour at bridge piers by a downstream bed sill. *JOURNAL OF HYDRAULIC ENGINEERING, 135*(1), 13-21.

Jalil, S. A. (2018). Analysis of the Modeling Outputs of Shape Factor Effect on Flow Structure between Bridge Piers. *Journal of University of Babylon for Engineering Sciences, 26*(4), 208-221.

Kirkil, G., Constantinescu, G., & Ettema, R. (2005). The horseshoe vortex system around a circular bridge pier on equilibrium scoured bed *Impacts of Global Climate Change* (pp. 1-12).

Klingeman, P. C. (1973). Hydrologic evaluations in bridge pier scour design. *Journal of the Hydraulics Division, 99*(12), 2175-2184.

Kumar, D., Yadav, H. L., & Himanshu, S. K. (2011). Estimation of scour depth around bridge piers by Using HEC-RAS. *Recent Advances in Civil Engineering, 421*, 425.

Lagasse, P. F. (2007). *Countermeasures to protect bridge piers from scour* (Vol. 593): Transportation Research Board.

Lauchlan, C. S., & Melville, B. W. (2001). Riprap protection at bridge piers. *JOURNAL OF HYDRAULIC ENGINEERING, 127*(5), 412-418.

Ladeinde, F., Alabi, K., Safta, C., Cai, X., & Johnson, F. (2006). The first high-order CFD simulation of aircraft: challenges and opportunities. In *44th AIAA Aerospace Sciences Meeting and Exhibit* (p. 1526).

Lu, J.-Y., Hong, J.-H., Su, C.-C., Wang, C.-Y., & Lai, J.-S. (2008). Field measurements and simulation of bridge scour depth variations during floods. *JOURNAL OF HYDRAULIC ENGINEERING, 134*(6), 810-821.

Melville, B., & Sutherland, A. (1988). Design method for local scour at bridge piers. *JOURNAL OF HYDRAULIC ENGINEERING, 114*(10), 1210-1226.

Melville, B. W. (1997). Pier and abutment scour: integrated approach. *JOURNAL OF HYDRAULIC ENGINEERING, 123*(2), 125-136.

Melville, B. W., & Coleman, S. E. (2000). *Bridge scour*: Water Resources Publication.

Mohammadi Givshad, S., Ramezani, Y., & Khozeymehnezhad, H. (2020). Investigation of scour around the dual bridge piers under unsteady flow conditions using experimental model. *Journal of Applied Research in Water and Wastewater, 7*(1), 57-63.

Moncada-M, A., Aguirre-Pe, J., Bolivar, J., & Flores, E. (2009). Scour protection of circular bridge piers with collars and slots. *Journal of Hydraulic Research, 47*(1), 119-126.

Moriasi, D. N., Arnold, J. G., Van Liew, M. W., Bingner, R. L., Harmel, R. D., & Veith, T. L. (2007). Model evaluation guidelines for systematic quantification of accuracy in watershed simulations. *Transactions of the ASABE, 50*(3), 885-900.

Mousavi, F., & Daneshfaraz, R. (2013). Evaluating various factors in calculation of scour depth around bridge piers using HEC-RAS Software, CSU2001 and Froehlich equations. *Journal of Civil Engineering and Urbanism, 3*(6), 398-402.

Neill, C. (1978). LOCAL SCOUR AROUND PIERS: Journal of Hydraulic Research, Vol. 15, No. 3, 1977.

Raudkivi, A. J., & Ettema, R. (1977). Effect of sediment gradation on clear water scour. *Journal of the Hydraulics Division, 103*(10), 1209-1213.

Richardson, A. E. (2001). Prospects for using soil microorganisms to improve the acquisition of phosphorus by plants. *Functional Plant Biology*, *28*(9), 897-906.

CURRICULUM VITAE

Mohammed Ali Obiad

EDUCATION

2021-2023 **Master Degree in Civil Engineering**

Gaziantep University, Gaziantep, Türkiye

2012-2018 **Bachelor in Civil Engineering**

Tikrit University